

Discovery and Biological Evaluation of a Novel Class of Dual Microsomal Prostaglandin E₂ Synthase-1/5-lipoxygenase Inhibitors Based on 2-[(4,6-Diphenethoxy)pyrimidin-2-yl]thio]hexanoic Acid

Martina Hieke,^{†,‡} Christine Greiner,^{§,‡} Michaela Dittrich,[†] Felix Reisen,[⊥] Gisbert Schneider,[⊥] Manfred Schubert-Zsilavecz,^{*,†} and Oliver Werz^{*,||}

[†]Institute of Pharmaceutical Chemistry, ZAFES/LiFF/Goethe-University Frankfurt, Max-von-Laue-Str. 9, D-60438 Frankfurt am Main, Germany

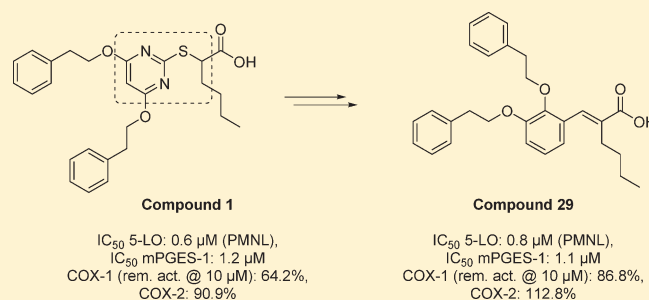
[§]Department of Pharmaceutical Analytics, Pharmaceutical Institute, Eberhard-Karls-University Tuebingen, Auf der Morgenstelle 8, D-72076 Tuebingen, Germany

[⊥]Department of Chemistry and Applied Biosciences, Swiss Federal Institute of Technology (ETH), Zurich, Switzerland

^{||}Chair of Pharmaceutical/Medicinal Chemistry, Institute of Pharmacy, Friedrich-Schiller-University Jena, Philosophenweg 14, D-07743 Jena, Germany

S Supporting Information

ABSTRACT: Various inflammatory diseases are associated with the excessive formation of leukotrienes (LTs) and prostaglandins (PGs). Herein, we present a novel class of dual inhibitors of 5-lipoxygenase (5-LO) and microsomal prostaglandin E₂ synthase-1 (mPGES-1), key enzymes in the formation of LTs and PGE₂, respectively. On the basis of the structure of 2-[(4,6-diphenethoxy)pyrimidin-2-yl]thio]hexanoic acid (**1**), we performed a detailed SAR analysis, and mechanistic studies were carried out to elucidate the mode of 5-LO inhibition. Interestingly, the pyrimidine ring including the thioether of **1** could be replaced by a simple benzyl or a benzylidene moiety yielding a novel series of bioactive 2-benzylidene- and 2-benzylhexanoic acids exemplified by 2-(2,3-diphenethoxybenzylidene)hexanoic acid, **29** (IC₅₀ 5-LO = 0.8 μM; mPGES-1 = 1.1 μM). Importantly, none of the novel bioactive derivatives strongly inhibited cyclooxygenase activities. Together, we provide novel promising lead compounds for the treatment of inflammatory diseases valuable for further investigations *in vivo*.



INTRODUCTION

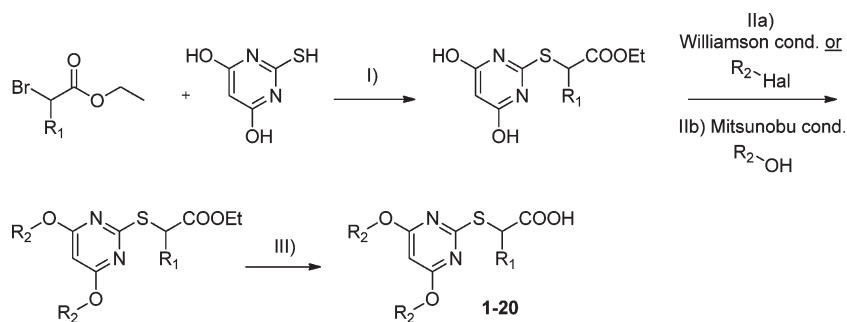
Leukotrienes (LTs) and prostaglandins (PGs) represent potent lipid mediators that are involved in inflammatory processes. They contribute to fever, pain, and allergic diseases and play a crucial role in cardiovascular diseases (CVD) and various types of cancer.^{1–3} The first step in the biosynthesis of both groups of eicosanoids is the release of arachidonic acid (AA) from phospholipids of cellular membranes by cytosolic phospholipase A₂ (cPLA₂). Subsequently, AA is converted into LTA₄ by 5-lipoxygenase (5-LO) or into PGH₂ by two different isoforms of cyclooxygenase (COX). LTA₄ is then metabolized by LTA₄ hydrolase into the chemotactic LTB₄ or by LTC₄ synthase into cysteinyl leukotrienes (LTC₄, LTD₄, and LTE₄), which evoke bronchoconstriction and increase vascular permeability.^{2,4}

COX-1 is constitutively expressed and involved in the biosynthesis of physiologically important PGs (e.g., TXA₂, PGE₂, PGI₂, PGF_{2α}) with house-keeping functions. In contrast, COX-2 is an inducible isoenzyme and up-regulated during inflammatory processes.⁴ COX-2 derived PGH₂ is efficiently transformed into

the pro-inflammatory PGE₂ by the inducible microsomal prostaglandin E₂ synthase (mPGES)-1. Nonsteroidal anti-inflammatory drugs (NSAIDs), which inhibit the activity of both COX isoenzymes, as well as selective COX-2 inhibitors (coxibs), are widely used in the therapy of pain and inflammatory diseases. Nevertheless, NSAIDs provoke severe side effects in the gastrointestinal tract due to suppression of gastroprotective (mainly COX-1-derived) PGE₂ and elevated LTB₄ levels.⁵ Moreover, the suppression of prostanoid biosynthesis also causes dysfunction of the kidney (NSAIDs) and cardiovascular toxicity (coxibs), the latter due to an imbalance of beneficial prostacyclin and detrimental thromboxane A₂. Hence, exclusive inhibition of massive (COX-2-derived) PGE₂ formation combined with perpetuation of homeostatic PGs would be desirable. Moreover, based on the pro-inflammatory function of LTs and the unwanted effects of elevated LTs in the gastrointestinal and the cardiovascular

Received: January 27, 2011

Published: May 18, 2011

Scheme 1. Synthesis of Thiobarbituric Acid Derivatives 1–20^a

^a Reagents and conditions: (I) α -bromo-(R_1)-ethyl acetate (1.5 equiv), thiobarbituric acid (1 equiv), TEA (1.5 equiv), DMF, 80 °C, 4 h; (IIa) precursor resulting from step I (1 equiv), R_2 -Hal (2.1 equiv), K_2CO_3 (2.3 equiv), DMF, 80 °C, 3–28 h or (IIb) precursor resulting from step I (1 equiv), R_2 -OH (2 equiv), diethyl azodicarboxylate (DEAD; 2.5 equiv), TPP (2.5 equiv), THF, rt, 1–3 h; (III) precursor resulting from step II (1 equiv), $LiOH \cdot H_2O$ (5 equiv), THF/MeOH, H_2O , 25–50 °C, 2–24 h.

system, dual inhibition of mPGES-1 and 5-LO might be even more efficient with less side effects than interference with one single pathway.⁵

While there is little known about factors influencing mPGES-1 activity in the cell, the activity of 5-LO is modulated by various cofactors,⁶ which may also influence the susceptibility toward pharmacological inhibitors.^{7,8} Thus, 5-LO activity is controlled by phosphorylations at serine residues, Ca^{2+} , ATP, coactosin-like protein (CLP), phospholipids, and glycerides.⁹ Despite considerable research efforts, zileuton is still the only 5-LO inhibitor that has succeeded clinical trials and reached the market. The lack of selectivity or mechanism-based side effects were the main reasons for the failure of 5-LO inhibitors as drug candidates in clinical trials. Therefore, we included various cell-based and cell-free assays in our studies to address mechanistic aspects of 5-LO inhibition by one of the lead compounds.

Herein, we present a novel class of dual inhibitors of human mPGES-1 and 5-LO. In previous studies, we found that a series of α -substituted pirinixic acid derivatives inhibited mPGES-1 and 5-LO *in vitro*, and the respective lead compound, 2-(4-chloro-6-(2,3-dimethylphenylamino)pyrimidin-2-ylthio)octanoic acid (YS121), exhibited anti-inflammatory efficacy *in vivo*.^{10,11} Of interest, some of these α -substituted pirinixic acid derivatives also modulated γ -secretase and peroxisome proliferator-activated receptor γ (PPAR γ), such as the 2-[(4,6-diphenethoxy-pyrimidin-2-yl)thio]hexanoic acid **1**.¹² Based on the structure of compound **1**, a comprehensive structure–activity relationship (SAR) study for human mPGES-1 and 5-LO was executed. Aiming to identify novel, more simplified structural scaffolds, we performed broad structural variations in the α -position of the carboxylic acid as well as on the pyrimidine core. To this end, we established a synthetic method that enabled the development of a structurally different class of bioactive compounds containing a trisubstituted benzene scaffold as central part of the molecule.

RESULTS AND DISCUSSION

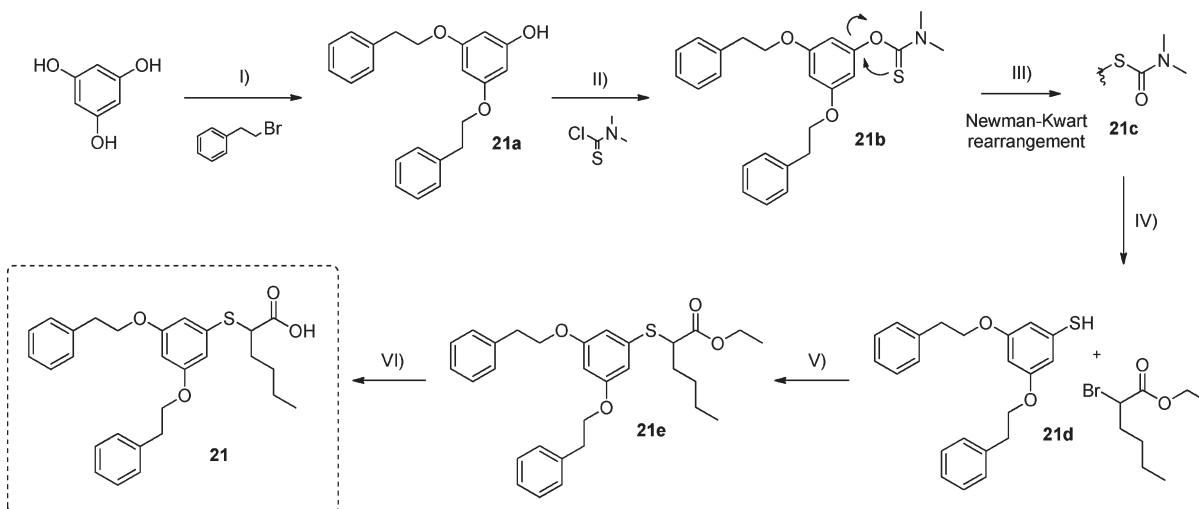
Chemistry. Preparation of thiobarbituric acid derivatives **1–20** is outlined in Scheme 1 and was described previously.¹² First, the respective α -bromo- R_1 -acetate and thiobarbituric acid were combined via a nucleophilic substitution. Next, the two lipophilic moieties were introduced either by a Williamson-like or a Mitsunobu ether synthesis, and finally, the ester group was hydrolyzed to give the carboxylic acids **1–20**.

Preparation of 2-[(3,5-diphenethoxyphenyl)thio]hexanoic acid (**21**) was carried out in six steps (Scheme 2). The synthesis starts with the etherification of two hydroxyl groups of phloroglucinol.¹³ The resulting precursor **21a** was isolated in low yield from a mixture of mono-, di-, and trisubstituted phloroglucinol ethers. The third hydroxyl group was afterward activated with dimethylthiocarbamoyl chloride to obtain precursor **21b**. Heating at 240 °C led to a Newman–Kwart rearrangement yielding the protected thiol derivative **21c**, which was subsequently deprotected with NaOH to give **21d**.¹⁴ Finally, a reaction of **21d** and α -bromo ethylhexanoate resulted in the ester derivative **21e**, which was afterward hydrolyzed to the carboxylic acid **21**.

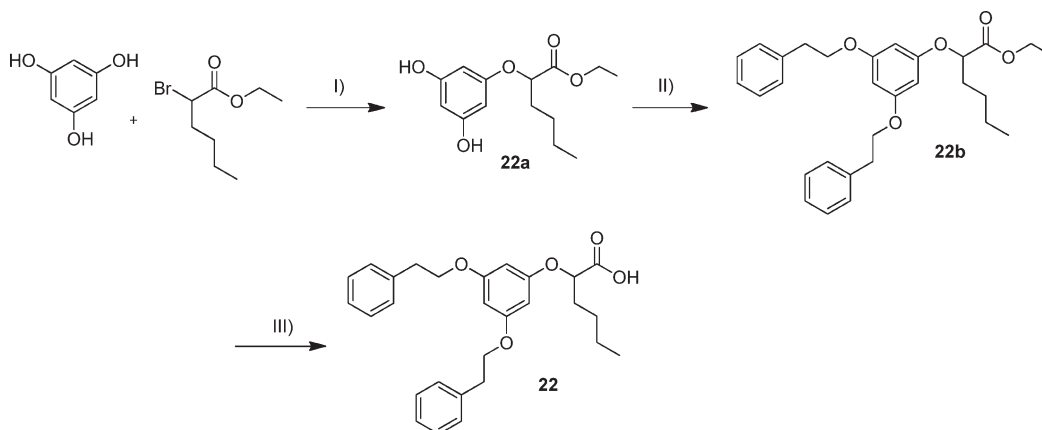
2-(3,5-Diphenethoxyphenoxy)hexanoic acid (**22**) was synthesized in three steps (Scheme 3). Starting with phloroglucinol, one hydroxyl group was etherified with α -bromo ethylhexanoate.¹³ Afterward, the two remaining hydroxyl groups were etherified via Mitsunobu synthesis. Finally, the ester group was hydrolyzed to yield the product **22**.

Disubstituted 2-benzylhexanoic acid and 2-benzylidenehexanoic acid derivatives **23–34** were prepared in four to five steps as shown in Scheme 4.¹⁵ Step one was an Arbuzov reaction between triethylphosphite and α -bromo ethylhexanoate yielding phosphonate precursor **A**. Second, the respective dihydroxybenzaldehyde was etherified in one or two steps under Williamson-like or Mitsunobu conditions to yield precursor molecules **23b**, **25b–28b**, and **31b–34b**. Subsequently, **23b**, **25b–28b**, and **31b–34b** were converted with phosphonate precursor **A** to an ester derivative in a Wittig–Horner reaction. Afterward, either the resulting precursors **23c**, **25c–28c**, and **31c–34c** were directly hydrolyzed to yield 2-benzylidenehexanoic acid derivatives or the double bond was hydrogenated using Pd/C and H_2 and the resulting product was finally hydrolyzed to yield 2-benzylhexanoic acid derivatives (compounds **23–34**).

Biological assays. All compounds synthesized within this study were characterized for their effects on the activity of human 5-LO and mPGES-1. As shown previously, none of the compounds **1–20** showed cytotoxic effects up to 50 μM ,¹² providing a high safety index for the identified lead compounds. Similarly, analysis of compounds **21–34** (at 10 μM final concentration) for acute cytotoxic effects, reflecting the conditions during the 30 min preincubation for 5-LO activity studies in polymorphonuclear leukocytes (PMNL), excluded significant cytotoxicity of the test compounds.

Scheme 2. Synthesis of 2-[(3,5-diphenethoxyphenyl)thio]hexanoic acid **21**^a

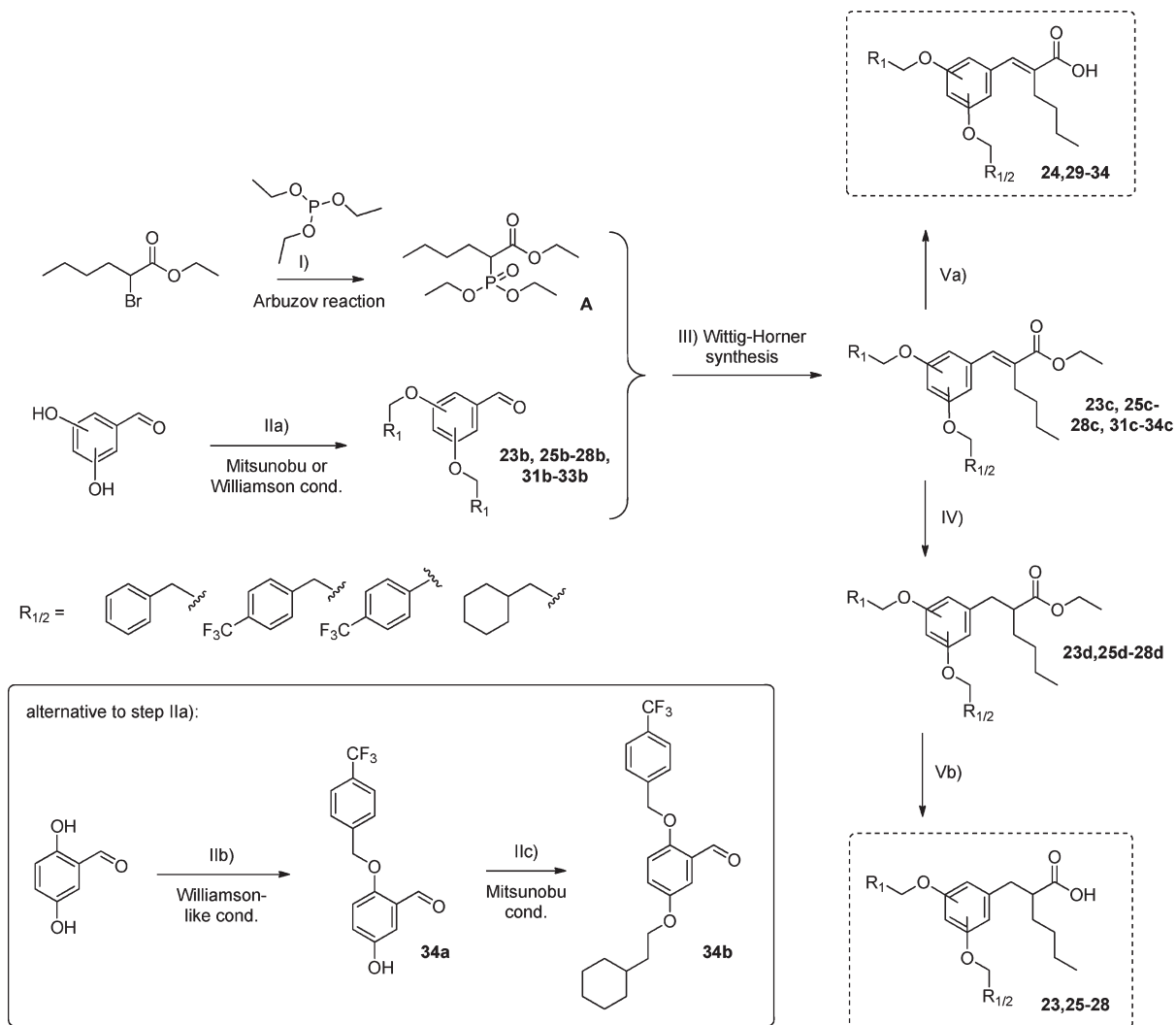
^a Reagents and conditions: (I) phloroglucinol (1.0 equiv), phenylethyl bromide (2.1 equiv), NaH (3 equiv), DMF (q.s.), rt, 20 h; (II) **21a** (1 equiv), dimethylthiocarbamoyl chloride (1.0 equiv), NaH (1.2 equiv), DMF (q.s.), 60 °C, 5 h; (III) **21b**, solvent-free, 240 °C, 5 h; (IV) **21c** (1.0 equiv), NaOH (1 mol/L; 10 mL), THF–MeOH, 80 °C, 3 h; (V) **21d** (1.0 equiv), α -bromo ethylhexanoate (1.2 equiv), NaH (1.2 equiv), DMF (q.s.), rt, 3 h; (VI) **21e** (1.0 equiv), LiOH·H₂O (5.0 equiv), THF–H₂O, 50 °C, 3 h.

Scheme 3. Synthesis of 2-(3,5-diphenethoxyphenoxy)hexanoic acid **22**^a

^a Reagents and conditions: (I) phloroglucinol (1.0 equiv), NaH (1.6 equiv), α -bromo ethylhexanoate (0.8 equiv), DMF (q.s.), rt, 8 h; (II) **22a** (1.0 equiv), phenylethanol (2.1 equiv), DEAD (2.5 equiv), TPP (2.5 equiv), THF, rt, 4 h; (III) **22b** (1.0 equiv), LiOH·H₂O (5.0 equiv), THF–H₂O, 50 °C, 24 h.

A detailed description of the methods for analysis of inhibition of 5-LO and mPGES-1 according to Koeberle et al.¹⁰ is summarized in the Materials and Methods. In brief, inhibition of 5-LO product formation was analyzed in a cell-based assay using PMNL, as well as in a cell-free assay using purified human recombinant 5-LO enzyme.¹⁶ Because a given test compound may suppress 5-LO product synthesis in intact cells without inhibiting 5-LO directly, for example, by interference with cofactors regulating 5-LO in the cell or with other enzymes involved in LT synthesis (e.g., FLAP, LTA₄H, LTC₄S), we analyzed all compounds for inhibition of isolated 5-LO as well. On the other hand, since many compounds inhibit 5-LO in cell-free assays but fail in intact cells for various reasons,⁷ we performed the cell-based assay and the cell-free assay side by side. Inhibition of mPGES-1 activity (transformation of PGH₂ to

PGE₂) was assessed in a cell-free assay using the mitochondrial fraction of IL-1 β -stimulated A549 lung epithelial adenocarcinoma cells and 20 μ M PGH₂ as substrate.¹⁷ In contrast to 5-LO synthesis inhibitors, for mPGES-1 inhibitors a cell-based test system that allows selective analysis of interference with endogenous mPGES-1 activity in the cell (i.e., the transformation of PGH₂ to PGE₂) is not available. Nevertheless, we addressed the ability of test compounds to interfere with COX enzymes that are committed in PGE₂ biosynthesis from the precursor AA. Inhibition of COX was analyzed in a cell-free assay using isolated ovine COX-1 and isolated human recombinant COX-2 enzymes.¹⁸ As reference compounds, the 5-LO inhibitor **35** (BWA4C, (*E*)-*N*-hydroxy-*N*-(3-(3-phenoxyphenyl)-allyl)acetamide),¹⁹ the mPGES-1 inhibitor **36** (MK-886, 3-(3-(*tert*-butylthio)-1-(4-chlorobenzyl)-5-isopropyl-1*H*-indol-2-yl)-2,2-dimethylpropanoic acid),²⁰ the

Scheme 4. Synthesis of Disubstituted 2-Benzylhexanoic Acid and 2-Benzylidenehexanoic Acid Derivatives 23–34.^a

^a Reagents and conditions: (I) triethylphosphite (1 equiv), α -bromo ethylhexanoate (1 equiv), 120 °C, 12 h; (IIa) dihydroxybenzaldehyde (1 equiv), R_1 -OH (2.1 equiv), TPP (2.5 equiv), DEAD (2.5 equiv), THF, rt, 1.4–24 h or 2,5-dihydroxybenzaldehyde (1 equiv), 4-(trifluoromethyl)benzylbromide (1.2 equiv), $CsCO_3$ (1.2 equiv), DMF, 50 °C, 5 h; (IIb) 2,5-dihydroxybenzaldehyde (1 equiv), 4-(trifluoromethyl)benzylbromide (1.2 equiv), $CsCO_3$ (1.2 equiv), DMF, 50 °C, 5 h; (IIc) 34a (1 equiv), 2-cyclohexylethanol (1.1 equiv), TPP (1.2 equiv), DEAD (1.2 equiv), THF, rt. (III) A (1.3 equiv), 23b, 25b–28b, 31b–34b (1 equiv), NaH (1.3 equiv), THF, rt, 2–22 h; (IV) 23c, 25–28c, Pd/C (10%), ethanol, rt, 24 h; (V) 24c, 29–34c or 23d, 25–28d (1 equiv), $LiOH \cdot H_2O$ (5 equiv), THF– H_2O , 50–60 °C, 6–40 h.

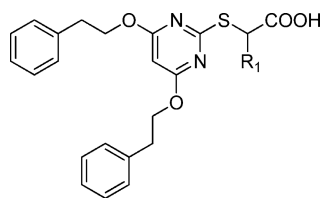
COX-1/2 inhibitor 37 (indomethacin, 2-[1-(4-chlorobenzoyl)-5-methoxy-2-methyl-1H-indol-3-yl]acetic acid), and the COX-2 inhibitor 38 (celecoxib, 4-(5-(4-methylphenyl)-3-(trifluoromethyl)pyrazol-1-yl)benzenesulfonamide) were used.

Structure–Activity Relationships of Dual Inhibitors of mPGES-1 and 5-LO. We have recently described the screening of dual mPGES-1/5-LO inhibitors based on pirinixic acid as basic structure. Within this study, three derivatives containing two phenethoxy residues at the pyrimidine ring (including compound 1) were synthesized and biologically characterized.¹⁰ Encouraged by the efficient inhibition of mPGES-1 ($IC_{50} = 1.2 \mu M$) and of 5-LO (cell-based $IC_{50} = 0.6 \mu M$, cell-free $IC_{50} = 4.7 \mu M$) by 2-[(4,6-diphenethoxypyrimidin-2-yl)thio]hexanoic acid, 1, we designed and synthesized a large set of compounds with broad modifications of all relevant structural features and performed SAR studies with respect to 5-LO and mPGES-1 inhibition.

The carboxylic acid moiety of compound 1 was not altered since the corresponding ester of 1 did not show significant effects on PGE_2 and 5-LO product formation at a concentration of 10 μM (remaining activity >80%, respectively; see Koeberle et al¹⁰).

The results, summarized in Tables 1–5, are expressed as IC_{50} values for all those compounds that inhibit mPGES-1 and 5-LO activity at 10 μM by more than 50%, for those with lower potency the remaining enzyme activities at 10 μM inhibitor concentrations are given. Concentrations >10 μM have not been considered due to solubility inconsistencies in aqueous assay buffers at higher concentrations of the test compounds. Starting from the lead 1, the importance of the aliphatic chain in α -position to the carboxylic acid was investigated by elongation or shortening of the α -*n*-butyl residue as well as by its replacement with a phenyl moiety. These modifications resulted in defined SARs for 5-LO and mPGES-1 (see Table 1). Whereas unsubstituted

Table 1. Structural Modification of the Substituents in α -Position of the Carboxylic Group and Resulting Effects on Inhibition of 5-LO and mPGES-1^a



Compound	R ₁	5-LO (IC ₅₀ [μM]; remaining activity at 10 μM)		mPGES-1 (IC ₅₀ [μM]; remaining activity at 10 μM)
		cell-based	cell-free	
1		0.6	4.7	1.2
2	-H	7.6	>10 57.0 ± 9.6%	> 10 66.4 ± 2.4%
3		2.8	9.0	7.3
4		0.4	2.8	2.0
5		0.8	4.9	1.2

^aData are expressed as mean ± SE; *n* = 3–4.

compound **2** and ethyl-substituted **3** were less potent on 5-LO in intact cells (IC₅₀ = 7.6 (**2**) and 2.8 μM (**3**)) compared with *n*-butyl-substituted **1** (IC₅₀ = 0.6 μM), the elongated α -*n*-hexyl derivative **4** and α -phenyl-substituted derivative **5** essentially retained high potency (IC₅₀ = 0.4 (**4**) and 0.8 μM (**5**)). Inhibition of 5-LO in the cell-free assay followed the same SARs as in intact cells, with about 3- to 8-fold reduced potency versus intact cells. The same SARs as for 5-LO are true also for mPGES-1 inhibition, because compound **4** (IC₅₀ = 2.0) with α -*n*-hexyl was similarly potent to α -*n*-butyl-substituted **1** and the same potency was obtained by the introduction of α -phenyl moiety (**5**). Thus, lipophilic bulky substituents in the α -position of the carboxylic group seemingly govern potency.

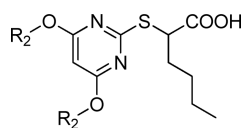
We used compound **1**, as the most potent dual 5-LO and mPGES-1 inhibitor, as template for further optimization. The two phenoxy moieties at the pyrimidine core forming a lipophilic backbone offer multiple opportunities for structural optimization. By shortening of the ethylene spacer connecting the phenyl moiety with the ether bridge via methylene in compound **6**, the potency for 5-LO and mPGES-1 inhibition was reduced (see Table 2). However, propylene (**7**) or butylene (**8**) spacers were tolerated, visualized by the submicromolar IC₅₀ values of 8 for 5-LO (cell-based) and mPGES-1 (0.7 and 0.9 μM, respectively).

Next, several electron-withdrawing (cyano (**9**), nitro (**10**), trifluoromethoxy (**11**), trifluoromethyl (**12**)) and -donating (methoxy (**13**) and methyl (**14**)) substituents were introduced in *para* position of the phenyl moieties of compound **1**. Additionally, both phenyl moieties of **1** were replaced by bioisosteric thiophene (**15**). As can be seen from Table 2, introduction

of *para*-substituents or replacement of phenyl by thiophene resulted in a subset of potent cellular 5-LO inhibitors (IC₅₀ = 0.3–0.7 μM). Among this set of compounds, the methoxy-substituted **13** is the most potent 5-LO inhibitor in intact cells. Concerning mPGES-1 inhibition, a correlation between the respective *para*-substituents and the potency was obvious. Thus, the introduction of trifluoromethyl (**12**, IC₅₀ = 1.9 μM) was well tolerated and especially a methyl moiety (**14**; IC₅₀ = 0.9 μM) retained the potency, whereas the corresponding trifluoromethoxy (**11**) or methoxy (**13**) groups markedly impaired the activity against mPGES-1. Electron-withdrawing cyano (**9**) and nitro (**10**) groups as well as replacement of phenyl by thiophene (**15**) impaired the potency as well.

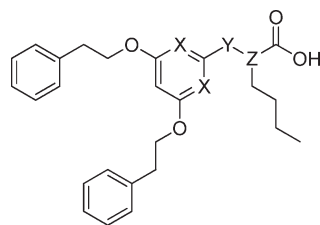
In addition, the phenyl moieties of the lipophilic backbone were replaced by aliphatic rings of various sizes (cycloheptyl (**16**), cyclohexyl (**17**), cyclopentyl (**18**), and cyclopropyl (**19**)), as well as by branched isopropyl (**20**) moieties. Introduction of cycloheptyl (**16**) and cyclopentyl rings (**18**) was beneficial neither for 5-LO (IC₅₀ cell-based = 2.4 (**16**) and 4 μM (**18**)) nor for mPGES-1 (IC₅₀ > 10 μM), whereas the intermediate sized cyclohexyl derivative **17** was quite potent with IC₅₀ values for 5-LO in PMNL = 0.8 μM and for mPGES-1 = 2.4 μM. Interestingly, the smaller isopropyl (**20**) and cyclopropyl moieties (**19**) are rather superior over the cyclopentyl-substituted **18**.

The second part of the SAR study focused on the impact of the central core scaffold of the compounds. Replacing the pyrimidine ring by a benzene moiety (while keeping the thioether of **1**) led to compound **21** that inhibited 5-LO almost equally well (IC₅₀ cell-based = 0.8 μM) as compound **1** (Table 3) and was somewhat less active on mPGES-1 (IC₅₀ = 4.6 μM). Moreover, replacement of

Table 2. Structural Modification of the Lipophilic Backbone and Resulting Effects on Inhibition of 5-LO and mPGES-1^a

Compound	R ₂	5-LO (IC ₅₀ [μM]; remaining activity at 10 μM)		mPGES-1 (IC ₅₀ [μM]; remaining activity at 10 μM)
		cell-based	cell-free	
Modification of ethylene spacers				
6		1.8	5.0	3.8
7		0.9	2.7	2.2
8		0.7	2.2	0.9
Introduction of para-substituents				
9		0.7	6.6	5.9
10		0.5	2.8	3.7
11		0.5	> 10 56.4 ± 13.3%	> 10 88.3 ± 6.3%
12		0.5	2.2	1.9
13		0.3	7.0	> 10 63.7 ± 7.4%
14		0.5	3.1	0.9
15		0.6	9.3	6.5
Replacement of phenyl by different aliphatic moieties				
16		2.4	> 10 53.8 ± 11.0%	> 10 62.4 ± 8.4%
17		0.8	9.0	2.4
18		4.0	6.8	> 10 90.0 ± 11.4%
19		1.2	9.3	9.6
20		1.2	6.8	> 10 54.5 ± 12.2%

^a Data are expressed as mean ± SE; *n* = 3–4.

Table 3. Variation of the Central Core Scaffold and Resulting Effects on Inhibition of 5-LO and mPGES-1^a

Compound	X	Y	Z	5-LO (IC ₅₀ [μM]; remaining activity at 10 μM)		mPGES-1 (IC ₅₀ [μM])
				cell-based	cell-free	
1	N	S	CH	0.6	4.7	1.2
21	CH	S	CH	0.8	7.2	4.6
22	CH	O	CH	0.6	> 10 60.0 ± 15.0%	3.4
23	CH	CH ₂ -	CH	4.7	> 10 80.3 ± 13.5%	2.4
24	CH	CH=	C	0.7	> 10 62.7 ± 17.6%	2.8

^aData are expressed as mean ± SE; *n* = 3–4.

the thioether of compound **21** by an ether moiety (compound **22**) even further (although marginally) improved the potency against 5-LO in PMNL (IC₅₀ = 0.6 μM) and mPGES-1 (IC₅₀ = 3.4 μM) versus **21**. Finally, exchange of the thioether by a methylene bridge, that is, replacement of all three heteroatoms of **1** with a pure carbon scaffold (2-(3,5-diphenethoxybenzyl)hexanoic acid, **23**) was essentially tolerated versus **1** with respect to mPGES-1 (IC₅₀ = 2.4 μM), whereas for 5-LO in PMNL a loss of potency was evident (IC₅₀ = 4.7 μM). Accordingly, the presence of a heteroatom (e.g., sulfur or oxygen), bridging the α-position and the aromatic ring, is not essential but at least governs bioactivity against 5-LO. Nevertheless, it was possible to restore the potent 5-LO inhibition of **1** by keeping the α-carbon atom but forming an ethenyl group (i.e., 2-(3,5-diphenethoxybenzylidene)hexanoic acid, **24**) which could be prepared within the same synthetic route as **23**. We therefore conclude that the steric configuration in this area in a fixed position might be favorable.

Based on the modified synthetic procedure of compound **23**, the variation of the two 3,5-diphenethoxy-substitution pattern was possible, and the respective 2,3- (**25**), 3,4- (**26**), 2,4- (**27**), and 2,5- (**28**) diphenethoxy-substituted 2-benzylhexanoic acid derivatives were prepared (see Table 4). Interestingly, shifting the two phenethoxy moieties from 3,5- to 2,4-positions (**27**) led to inactivity on both targets (remaining activity of 5-LO/mPGES-1 at 10 μM > 90%). 2,3-Substituted (**25**) and 3,4-substituted (**26**) compounds were about equally active compared with 3,5-diphenethoxy-substituted **23**. The most potent dual 5-LO and mPGES-1 inhibitor from this set turned out to be the 2,5-diphenethoxy-substituted compound **28** (IC₅₀ 5-LO = 0.9 μM

in PMNL, mPGES-1 = 2.4 μM). Additionally, we prepared the corresponding 2-benzylidenehexanoic acid analogues of **25** and **28**, that is, the 2-(2,3-diphenethoxybenzylidene)hexanoic acid, **29**, and 2-(2,5-diphenethoxybenzylidene)hexanoic acid, **30**, respectively. In fact, replacement of the ethylene by an ethenyl group enhanced the potency for **29** (IC₅₀ 5-LO cell-based = 0.8 μM; mPGES-1 = 1.1 μM) against both 5-LO and mPGES-1.

In order to further improve the efficiency, the phenethoxy residues of compound **30** (IC₅₀ 5-LO cell-based = 0.9 μM; mPGES-1 = 1.5 μM) were modified (Table 5). Replacement of the phenyl moieties in **30** by cyclohexyl (**31**) hardly altered the efficiency. However, substitution of the phenyl moieties by trifluoromethyl residues in *para*-position (**32**) enhanced the potency against 5-LO in PMNL (IC₅₀ = 0.3 μM). Shortening the ethylene linker between phenyl and the ether moiety of **32** to methylene (**33**) was tolerated with respect to 5-LO but the potency against mPGES-1 was lost. Also, compound **34** carrying one *p*-(trifluoromethyl)benzyloxy substituent and one cyclohexylethoxy residue was not active against mPGES-1 but efficiently inhibited 5-LO. Data of the reference inhibitors of 5-LO (compound **35**) and mPGES-1 (compound **36**) are given at the end of the table, and on the basis of the resulting effects of these compounds that correspond to the values from literature,^{19,20} we conclude that our results obtained for the novel compounds **1** to **34** are valid.

Inhibition of COX Enzymes. Inhibition of COX-1/2 by compounds **1**–**20** was examined before;¹² compounds **21**–**37** were assayed in the COX activity test systems, and the results are reported in Table 6. Inhibition of isolated ovine COX-1 and human recombinant COX-2 was determined and expressed as

Table 4. Variation of the Substitution Pattern of the Central Benzene Ring and Resulting Effects on Inhibition of 5-LO and mPGES-1^a

Compound	Structure	5-LO (IC ₅₀ [μM]; remaining activity at 10 μM)		mPGES-1 (IC ₅₀ [μM]; remaining activity at 10 μM)
		cell-based	cell-free	
23		4.7	> 10 80.3 ± 13.5%	2.4
25		2.1	4.9	3.9
26		6.0	> 10 54.0 ± 5.7%	2.7
27		> 10 98.1 ± 1.4%	> 10 85.6 ± 4.4%	> 10 90.1 ± 8.3%
28		0.9	> 10 65.5 ± 9.9%	2.4
29		0.8	> 10 91.3 ± 10.5%	1.1
30		0.9	> 10 78.2 ± 9.4%	1.5

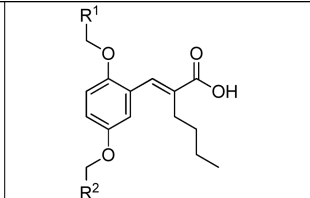
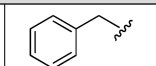
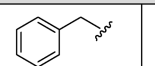
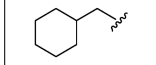
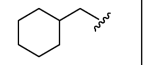
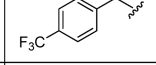
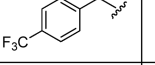
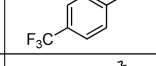
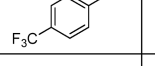
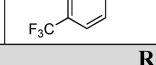
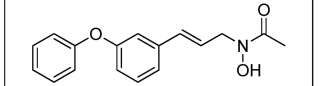
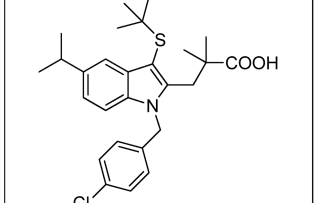
^aData are expressed as mean ± SE; *n* = 3–4.

remaining activity. In brief, the remaining COX-1 and COX-2 activities are higher than 50% for all compounds tested at a concentration of 10 μM. Thus, with respect to the high potency of the identified lead compounds against 5-LO and mPGES-1 (e.g., 1, 4, 8, 14, and 29), the concentrations needed for half-maximal

inhibition of COX enzymes are at least 10-fold higher than those for dual mPGES-1 and 5-LO inhibition.

Analysis of the Molecular Pharmacology of 2-[(4,6-Diphenethoxy)pyrimidin-2-yl]thio]octanoic Acid, 4. As shown above, 5-LO inhibition for all of the 34 test compounds was

Table 5. Variation of the Lipophilic Backbone of Compound 30 and Resulting Effects on Inhibition of 5-LO and mPGES-1^a

Compound			5-LO (IC ₅₀ [μM]; remaining activity at 10 μM)		mPGES-1 (IC ₅₀ [μM]; remaining activity at 10 μM)
	R ₁	R ₂	cell-based	cell-free	
Variations based on compound 30					
30			0.9	> 10 78.2 ± 9.4%	1.5
31			0.8	> 10 73.0 ± 10.6%	3.4
32			0.3	> 10 55.6 ± 2.7%	3.5
33			0.2	4.4	> 10 55.1 ± 5.4%
34			0.4	> 10 55.5 ± 7.9%	> 10 74.0 ± 9.4%
Reference inhibitors of 5-LO and mPGES-1					
35			0.08	0.16	not determined
36			0.09	no inhibition at 1 μM	2.4

^aData are expressed as mean ± SE; *n* = 3–4.

superior in the cell-based test system compared with the cell-free assay, and for some compounds, for example, **11**, **13**, **22**, **32**, and **34**, the IC₅₀ values were even more than 20-fold higher in the cell-free versus the cell-based assay. Hence, the compounds act as direct 5-LO inhibitors, but apparently factors in intact cells govern the potency, or alternatively, the compounds may primarily (and potentially) suppress cellular 5-LO product synthesis by other additional mechanisms than direct interference with 5-LO.

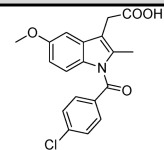
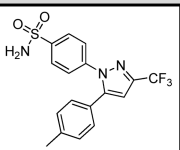
To further investigate the underlying mechanism of inhibition of cellular 5-LO product synthesis, we performed mechanistic studies with compound **4** (one of the most effective 5-LO inhibitors in cell-free and cell-based assays from our SAR investigations), applying particular experimental settings. In order to assess the selectivity of **4** for 5-LO, we investigated the effects of **4** on the activity of 12/15-LO (15-LO-1), expressed in eosinophilic granulocytes, and of platelet-type-12-LO derived from PMNL-adherent platelets. The amount of 15(*S*)-hydro(pero)xy-5,8,11-*cis*-13-*trans*-eicosatetraenoic acid (15(*S*)-H(p)ETE), formed by 12/15-LO, and 12(*S*)-hydro(pero)xy-5,8-*cis*-10-*trans*-14-*cis*-eicosatetraenoic acid (12(*S*)-H(p)ETE), formed

by p12-LO, was rather augmented after treatment with **4** (Figure 1A), and a similar pattern could be observed for the reference 5-LO inhibitor **38** (not shown).

In view of the structural features, no redox- or iron chelating activities are evident for compound **4** and its analogues, and in a radical scavenger assay, **4** up to 100 μM failed to reduce 1,1-diphenyl-2-picrylhydrazyl (DPPH) in contrast to ascorbic acid and L-cystein (data not shown). Moreover, wash-out experiments (dilution from 3 to 0.3 μM) demonstrated that the inhibitory effect of **4** on isolated 5-LO can be reverted (not shown), implying that the compound does not irreversibly inactivate 5-LO or acts by covalent binding to it.

Previous studies showed that the inhibitory potency of some 5-LO inhibitors can vary depending on the stimulus used to evoke 5-LO product synthesis in PMNL.^{21,22} Therefore, besides induction of 5-LO product formation with A23187, we addressed 5-LO product formation also after stimulation of PMNL with 1 μM N-formyl-methionyl-leucyl-phenylalanine (fMLP) upon priming with 1 μg/mL lipopolysaccharide (LPS) leading to 5-LO activation via release of intracellular Ca²⁺ and phosphorylation

Table 6. COX Inhibition of the Compounds 1-34 at a Concentration of 10 μM^a

Com-Pound	COX-1 remaining activity [%] at 10 $\mu\text{M} \pm \text{SE}$	COX-2 remaining activity [%] at 10 $\mu\text{M} \pm \text{SE}$	Com-pound	COX-1 remaining activity [%] at 10 $\mu\text{M} \pm \text{SE}$	COX-2 remaining activity [%] at 10 $\mu\text{M} \pm \text{SE}$
1	64.2 (\pm 8.8)	90.9 (\pm 10.2)	11	73.0 (\pm 6.7)	75.8 (\pm 5.0)
2	91.8 (\pm 2.8)	91.7 (\pm 7.8)	12	54.4 (\pm 10.6)	69.0 (\pm 12.4)
3	84.6 (\pm 3.2)	56.9 (\pm 0.8)	13	72.8 (\pm 10.3)	94.6 (\pm 13.5)
4	61.8 (\pm 9.8)	63.8 (\pm 9.7)	14	57.2 (\pm 7.3)	93.3 (\pm 11.6)
5	72.2 (\pm 7.7)	86.0 (\pm 12.6)	15	76.6 (\pm 4.0)	102.4 (\pm 7.3)
6	88.9 (\pm 12.3)	61.6 (\pm 1.4)	16	56.1 (\pm 5.1)	50.1 (\pm 2.1)
7	78.8 (\pm 8.6)	51.9 (\pm 6.5)	17	52.7 (\pm 6.4)	49.5 (\pm 10.7)
8	78.8 (\pm 8.1)	53.9 (\pm 8.2)	18	68.2 (\pm 4.0)	84.7 (\pm 2.0)
9	88.8 (\pm 9.6)	82.6 (\pm 14.1)	19	97.7 (\pm 8.7)	87.9 (\pm 3.4)
10	82.1 (\pm 7.0)	91.6 (\pm 8.4)	20	72.4 (\pm 11.8)	80.5 (\pm 11.4)
Replacement of central scaffold					
21	71.3 (\pm 2.1)	109.7 (\pm 4.9)	28	63.8 (\pm 16.6)	66.5 (\pm 11.0)
22	71.6 (\pm 3.7)	92.5 (\pm 2.7)	29	86.8 (\pm 24.3)	112.8 (\pm 21.9)
23	78.7 (\pm 12.9)	78.4 (\pm 11.9)	30	68.0 (\pm 12.1)	94.4 (\pm 10.7)
24	81.4 (\pm 8.5)	81.4 (\pm 8.9)	31	76.4 (\pm 7.3)	123.4 (\pm 19.5)
25	66.1 (\pm 9.8)	89.6 (\pm 13.4)	32	81.0 (\pm 11.8)	102.4 (\pm 7.3)
26	95.8 (\pm 21.7)	86.4 (\pm 11.8)	33	82.6 (\pm 4.7)	102.0 (\pm 5.5)
27	99.1 (\pm 12.1)	110.3 (\pm 5.8)	34	92.3 (\pm 9.2)	106.1 (\pm 11.9)
Reference compounds for COX-1 and COX-2 inhibition					
37 (indomethacin)		COX-1 26.6 (\pm 4.8)	38 (celecoxib)		COX-2 34.3 (\pm 10.4)

^aValues of compounds 1–20 were reported previously.¹² Data are given as mean \pm SE, $n = 3$. Reference inhibitors 37 (indomethacin) and 38 (celecoxib) are listed at the end of the table.

by mitogen-activated protein kinases (MAPK).²³ Indeed, the potency of 4 for inhibition of 5-LO product formation was somewhat impaired upon stimulation with LPS/fMLP compared with A23187 (Figure 1B). Activation of 5-LO by phosphorylation after applying cell stress (300 mM NaCl, together with 40 μM AA) occurs independent of Ca^{2+} ²⁴ and these conditions led to a slight loss of efficacy of 4 as well (Figure 1C). Conclusively, compound 4 is more efficient on 5-LO activated by Ca^{2+} rather than under conditions where phosphorylations by MAPK partially or fully activate 5-LO.

Next, we tested the influence of the substrate concentration on the 5-LO inhibitory effect of 4. Figure 1D demonstrates that the potency of 4 is reduced with increasing amounts of AA (20, 40, and 60 μM), suggesting that 4 may inhibit 5-LO in a competitive manner. A similar effect on the efficiency of the reference 35 was obvious, although the loss of potency did not depend on the various AA concentrations.

A major disadvantage of several non-redox-type 5-LO inhibitors is their dependence on reducing conditions.²¹ In fact, the 5-LO inhibitory effect of 4 in 100 000 \times g supernatants from

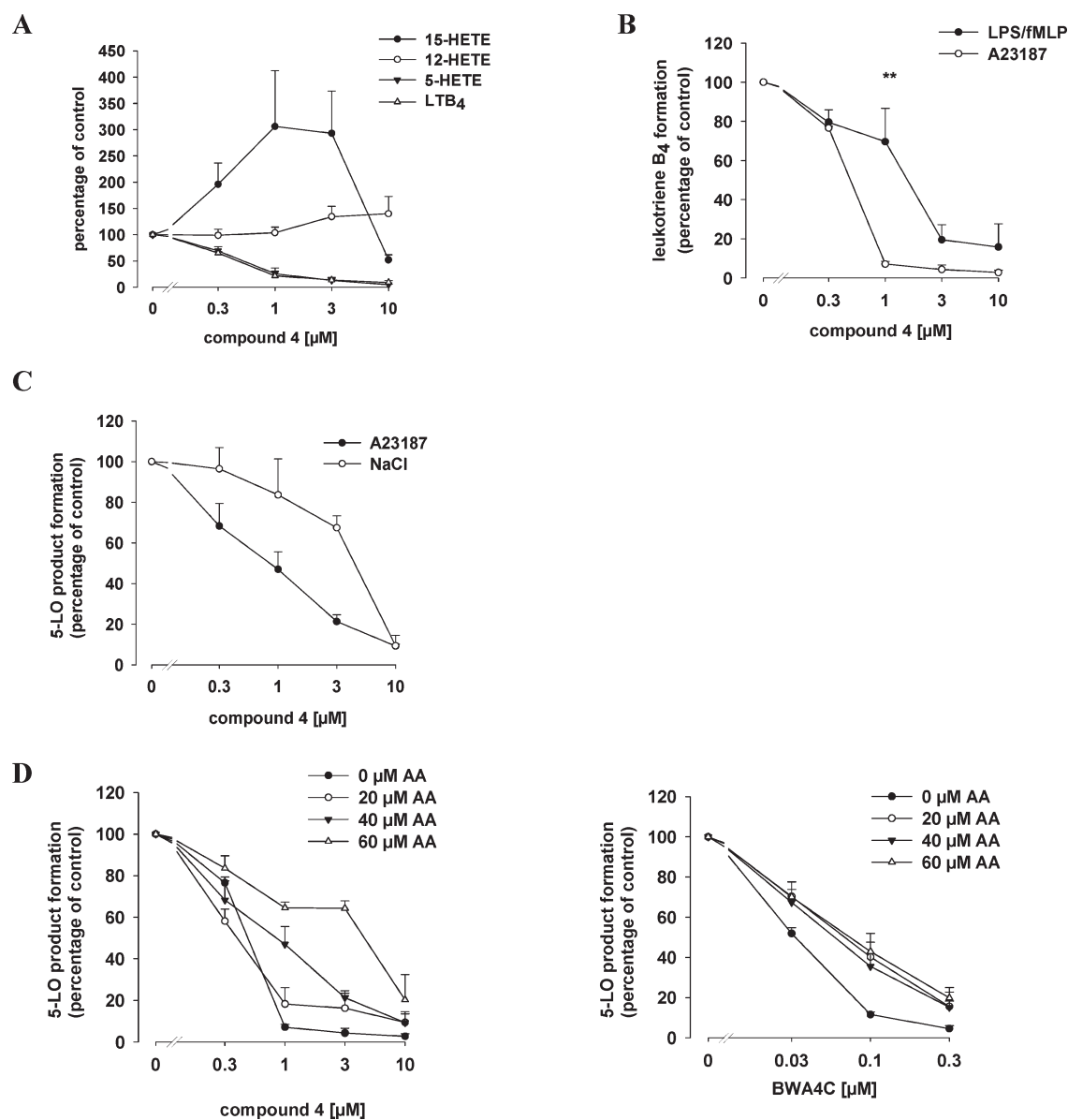


Figure 1. Effect of compound 4 on 5-LO product formation in PMNL. (A) Influence of compound 4 on 5-, 12-, and 15-LO product formation in A23187-stimulated PMNL (5×10^6 /mL) in the presence of $20 \mu\text{M}$ AA. The amounts of 15(S)-H(p)ETE, 12(S)-H(p)ETE, 5(S)-H(p)ETE, and LTB₄ were determined by HPLC. The 100% values correspond to 53.1 ± 13.0 ng/mL 15-H(p)ETE, 150.0 ± 36.4 ng/mL 12-H(p)ETE, 618.3 ± 55.6 ng/mL 5-H(p)ETE, and 85.1 ± 4.5 ng/mL LTB₄. Data are means \pm SEM, $n = 4$. (B) Effect of compound 4 on LTB₄ formation in A23187- and LPS/fMLP-stimulated PMNL (5×10^6 /mL). Cells were preincubated with 4 for 15 min at 37°C , and $2.5 \mu\text{M}$ A23187 was added. LTB₄ was determined by HPLC after 10 min incubation at 37°C . Alternatively, cells (2×10^7 /mL) were preincubated with 4 for 15 min at 37°C , primed with $1 \mu\text{g}/\text{mL}$ LPS, and then stimulated with $1 \mu\text{M}$ fMLP. After 5 min, the amount of released LTB₄ was determined by ELISA. The 100% values correspond to 189.2 ± 57.7 pg/mL LTB₄. Data are means \pm SEM, $n = 4$; $**p < 0.01$ vs controls that were stimulated with A23187, ANOVA + Tukey *post-hoc* test. (C) Efficiency of compound 4 under conditions that induce 5-LO product synthesis by A23187 or cell stress. PMNL (5×10^6 /mL) were preincubated with 4 for 15 min at 37°C . NaCl (0.3 M) was supplemented 3 min before addition of $40 \mu\text{M}$ AA; $2.5 \mu\text{M}$ A23187 was added together with $40 \mu\text{M}$ AA. After 10 min at 37°C , the reaction was stopped and 5-LO products were measured. The 100% values correspond to 529.4 ± 61.2 and 335.8 ± 50.0 ng/mL 5-LO products for cells stimulated by A23187 and by NaCl, respectively. Data are means \pm SEM, $n = 4$. (D) Efficiency of compounds 4 and 35 at variant substrate concentrations. PMNL (5×10^6 /mL) were preincubated with 4 or 35 for 15 min at 37°C , the indicated amounts of AA and $2.5 \mu\text{M}$ A23187 were added, and the reaction was stopped after 10 min to analyze 5-LO product formation: 199.2 ± 37.9 , 1136.7 ± 299.7 , 529.4 ± 61.2 and 498.4 ± 87.7 ng/mL 5-LO products at 0, 20, 40, and $60 \mu\text{M}$ AA, respectively. Data are means \pm SEM, $n = 3$.

PMNL homogenates ($S100$, $IC_{50} = 12.5 \mu\text{M}$) or on isolated 5-LO ($IC_{50} = 2.8 \mu\text{M}$) was significantly attenuated versus intact cells ($IC_{50} = 0.4 \mu\text{M}$), which was true also for the non-redox-type 5-LO inhibitors 1-ethyl-6-((3-fluoro-5-(4-methoxy-3,4,5,6-tetrahydro-2H-pyran-4-yl)phenoxy)methyl)-2-quinolone (ZM230487)²⁵

or 2-cyano-4-(3-furyl)-7-[[6-[3-(3-hydroxy-6,8-dioxabicyclo[3.2.1]octanyl)]-2-pyridyl]methoxy]-naphthalene (L-739.010).²¹ In contrast to these non-redox-type inhibitors, addition of 1 mM dithiothreitol (DTT, to reconstitute GPx activity and thus to create reducing conditions) did not restore potent 5-LO inhibition

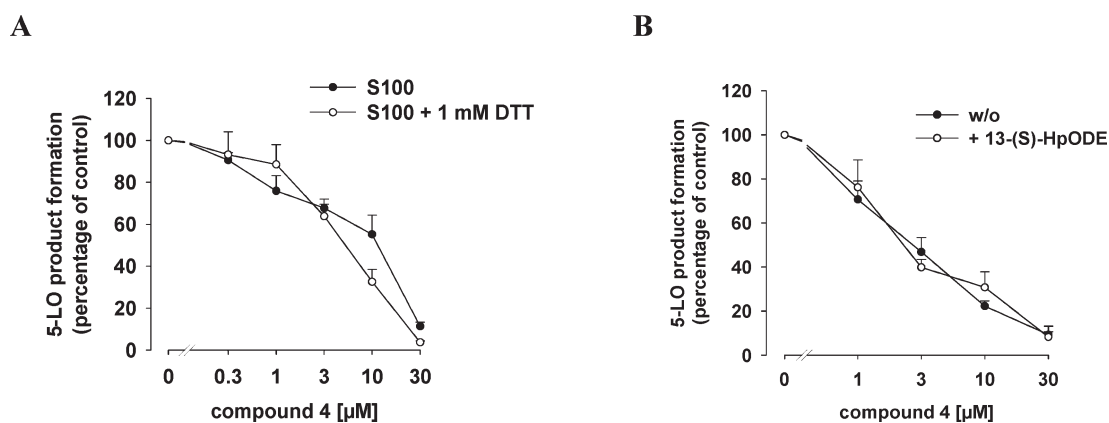


Figure 2. Influence of the redox tone on 5-LO inhibition by compound 4 in cell-free assays. (A) Influence of DTT. The S100 from homogenates of PMNL ($5 \times 10^6/\text{mL}$) was preincubated with compound 4 or with vehicle (0.3% DMSO) in the presence or absence of 1 mM DTT for 5–10 min at 4 °C. Then, samples were prewarmed at 37 °C for 30 s and 2 mM CaCl_2 and 20 μM AA were added, and after 10 min at 37 °C, 5-LO activity was analyzed by HPLC. The 100% values correspond to 765.2 ± 261.5 and 1044.8 ± 263.0 ng/mL 5-LO products in homogenates and in homogenates plus DTT, respectively. Data are means + SEM, $n = 3$. (B) Influence of 13(S)-HpODE. Purified 5-LO (0.5 $\mu\text{g}/\text{mL}$, human recombinant) was preincubated with 4 or with vehicle (0.3% DMSO) for 5–10 min at 4 °C. Samples were prewarmed at 37 °C for 30 s, and 5-LO product formation was started by addition of 2 mM CaCl_2 and 20 μM AA in the presence or absence of 1 μM 13(S)-HpODE. After another 10 min, 5-LO products were determined. The 100% values correspond to 923.4 ± 196.1 and 1373.9 ± 197.4 ng 5-LO products per 0.5 μg of enzyme in the absence and presence of 13(S)-HpODE, respectively. Data are means + SEM, $n = 3$.

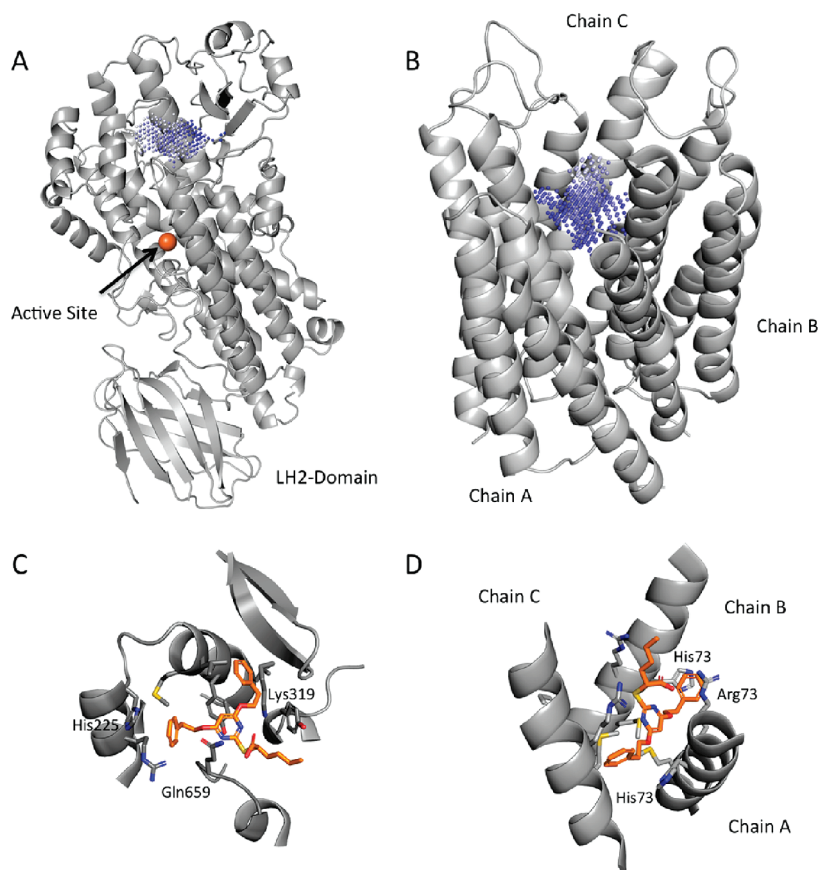


Figure 3. Computer-assisted protein binding site analysis. Potential binding sites for dual mPGES-1 and 5-LO inhibitors were predicted by PoLiMorph, as highlighted: (A) 5-LO (PDB-ID 3o8y) and (B) mPGES-1 (PDB-ID 3dww). Reasonable binding poses were obtained by automated ligand-docking, exemplarily shown for compound 1 in the pockets of (C) 5-LO and (D) mPGES-1.

in S100 (Figure 2A), suggesting that the potency of 4 is independent of the redox tone. Along these lines, inclusion of 1 μM

13(S)-HpODE in the cell-free assay using isolated 5-LO did not alter the potency of compound 4 (Figure 2B).

Computational Analysis of Potential Ligand Binding Sites.

In a preliminary attempt to identify potential ligand binding sites for dual 5-LO and mPGES-1 inhibitors, cavities on the surface of the two proteins were compared. First, potential binding sites of Protein Data Bank (PDB)²⁶ entries 3o8y²⁷ (5-LO, chain A) and 3dww²⁸ (mPGES-1) were extracted using our software PocketPicker.²⁹ For 5-LO, we found nine and for mPGES-1 six surface cavities exceeding a volume of 110 Å³ (less than 5% of all protein binding sites accommodating a ligand have a smaller volume; study performed on scPDB³⁰ v.2009, data not published). Then, pairwise comparisons between all identified cavities from mPGES-1 and 5-LO were performed. This was done with PoLiMorph,³¹ a software tool that is able to reveal related receptor–ligand interaction potentials even in the absence of protein sequence homology. Only one pocket pair from 5-LO and mPGES-1 achieved a similarity score greater than PoLiMorph's reliability threshold of 0.15.³¹ In 5-LO, this predicted binding site lies distant from the active site and the C2-like domain (Figure 3A). It is flanked by residues Arg²²¹, His²²⁵, Met²³⁰, Tyr²³⁴, Leu²³⁷, Lys³¹⁹, Tyr⁴⁶⁷, and Glu⁶⁵⁶. In mPGES-1, the respective predicted binding site is formed by residues His⁷¹, Arg⁷², and Met⁷⁶ from each of the three chains. Here, the pocket is located at the center of the protein structure where these residues come into close proximity (Figure 3B). Notably, both pockets contain an arginine–histidine–methionine triangle with similar edge lengths. To further elaborate the hypothesis that dual mPGES1/5-LO inhibitors might bind to these two pockets proposed by PoLiMorph, automated ligand docking studies were performed for compounds **1**, **2**, **5**, **13**, **14**, **29**, and **32** using the GOLD, v. 5.0.1, software in combination with the GOLDScore function.³² Favorable average docking score values of 81 (*stddev* = 7) for the predicted mPGES-1, and 79 (*stddev* = 3) for the predicted 5-LO binding site were obtained. These scores are statistically indistinguishable (Mann–Whitney U-test, *p* = 0.46), which points to actual pocket similarity. In comparison, docking of the compounds into the active site of 5-LO yielded significantly lower scores (*mean* = 61; *stddev* = 4; Mann–Whitney U-test: *p* < 0.001). Visual inspection of docking poses revealed reasonable conformations in both potential binding sites (Figure 3C,D). In the cavity of 5-LO, an aromatic face-to-face interaction between His²²⁵ and one of the two phenyl-residues of compound **1** is predicted, and the carboxylic group of compound **1** might act as a hydrogen-bridge acceptor for Lys³¹⁹ and Gln⁶⁵⁹ side chains. In the binding pocket of mPGES-1, aromatic face-to-face interactions seem feasible between both phenyl residues and His⁷² in chain A and His⁷² in chain B, respectively. Here, the carboxylic group acts as a potential hydrogen-bridge acceptor for Arg⁷³ in chain A. As a result of this computational study, we suggest that the two identified pockets might accommodate dual inhibitor **1**. The proposed interacting amino acid residues are candidates for mutation studies, which will help assess the validity of our hypothesis.

CONCLUSIONS

The therapeutic use of NSAIDs and coxibs against inflammatory diseases has become highly prevalent, although these classes of compounds possess critical target (i.e., COX)-related side effects resulting from the suppression of homeostatically relevant or protective PGs.⁴ Agents that dually inhibit the PGE₂ and the LT synthetic pathway are thought to be more efficient than traditional NSAIDs and, in particular, may also exhibit reduced

risk of side effects. Here, we describe the discovery of a novel class of potent dual inhibitors of 5-LO and mPGES-1 based on the structure of 2-[(4,6-diphenethoxy)pyrimidin-2-yl]thio]hexanoic acid, **1**, with minor influence on the activity of COX-1/2. Compound **14** is one of the most potent leads with a well-balanced activity against 5-LO (IC₅₀ cell-based = 0.5 μM) and mPGES-1 (IC₅₀ = 0.9 μM). Of interest, we established a new synthetic procedure allowing the replacement and broad modification of the central pyrimidine core of **1** in order to vary the phenethoxy positions at a central benzene ring with large space for structural optimization. Note that these 2-(diphenethoxybenzylidene)hexanoic acids constitute a novel structural class of dual mPGES-1/5-LO inhibitors with 2-(2,3-diphenethoxybenzylidene)hexanoic acid **29** (IC₅₀ 5-LO in PMNL = 0.8 μM; mPGES-1 = 1.1 μM) as the most potent representative from this set of compounds.

Evaluation of previous 5-LO inhibitors showed that complex regulation of 5-LO by various cofactors⁶ influences the susceptibility toward inhibitors and the efficiency of the compounds may strongly depend on experimental settings.^{7,8} Characterization in various cell-based and cell-free assays indicate that compound **4** shares characteristics with classical non-redox-type 5-LO inhibitors, including impaired potency when 5-LO is activated by phosphorylation events and the loss of efficiency at increased substrate concentrations.³³ However, **4** markedly inhibits 5-LO product formation also under nonreducing conditions, which is not the case for non-redox-type 5-LO inhibitors and thus encourages further studies. Taken together, we present different novel classes of compounds that dually act on 5-LO and mPGES-1 with minor activity on COX enzymes. Based on the overall suitable pharmacological profile, one may expect a synergistic anti-inflammatory activity along with unwanted side effects of traditional NSAIDs and coxibs. These data encourage for further pharmacological and pharmacokinetic studies in order to reveal the *in vivo* characteristics of the compounds in animal models.

MATERIALS AND METHODS

Compounds and Chemistry. The structures of previously reported compounds **1–20** were confirmed by ¹H and ¹³C NMR as well as by mass spectrometry (ESI); the purity (>95%) was determined by combustion analysis as described.¹² Compounds **21–34** were synthesized as described in Schemes 2–4. All commercial chemicals and solvents are of reagent grade and were used without further purification, unless otherwise specified. ¹H and ¹³C NMR spectra were measured in DMSO-*d*₆ or CDCl₃ on a Bruker ARX 300 or AV 300 spectrometer. Chemical shifts are reported in parts per million (ppm) using tetramethylsilane (TMS) as an internal standard. Mass spectra were obtained on a Fissous Instruments VG Platform 2 spectrometer measuring in the positive- or negative-ion mode (ESI-MS system). The purities of the final compounds were determined by combustion analysis, which has been performed by the Microanalytical Laboratory of the Institute of Organic Chemistry and Chemical Biology, Goethe-University Frankfurt, on a Foss Heraeus CHN-O-rapid elemental analyzer or an Elementar Vario Micro Cube. All compounds described here have a purity of 95% or higher. The synthetic procedure is described representatively for compounds **21**, **23**, and **24**. Detailed synthetic and analytical data of all compounds are provided in the Supporting Information.

Synthesis of 21 (2-[(3,5-Diphenethoxyphenyl)thio]hexanoic Acid) (Following Scheme 2). In method A (synthetic procedure of steps I, II, and V), sodium hydride (95%) was suspended in anhydrous DMF (q.s.) and stirred under argon atmosphere and ice bath cooling. Subsequently, E₁ was slowly added to the solution via syringe. After the

mixture was stirred for 30–60 min, E₂ was added, and the suspension was stirred at room temperature (steps I and V) or 60 °C (step II) until completed (TLC control). The mixture was then diluted with water and extracted two times with ethyl acetate. The organic fractions were dried over MgSO₄ and evaporated to yield the crude product. Purification was done by silica gel column chromatography using *n*-hexane/ethyl acetate to yield the pure products.

Step I, Synthesis of 21a (3,5-Diphenethoxyphenol)¹³. Method A: NaH (95%, 2.4 g, 90 mmol); E₁, phloroglucinol (3.78 g, 30 mmol); E₂, phenethyl bromide (11.7 g, 63 mmol); duration of synthesis, 20 h; product, orange solid; yield, 18.4% (1.84 g). ¹H NMR (300.13 MHz, (CD₃)₂SO): δ = 2.94–2.99 (t, 4H, J = 6.7 Hz, Ph'-CH₂), 4.05–4.13 (m, 4H, Ph-O-CH₂), 5.90–5.92 (m, 3H, Ph-H), 7.17–7.31 (m, 10H, Ph'-H), 9.37 (s, 1H, Ph-OH). ¹³C NMR (75.44 MHz, (CD₃)₂SO): δ = 34.86 (Ph'-CH₂), 67.38 (2C, Ph-O-CH₂), 92.30 (Ph-C₄), 94.65 (2C, Ph-C_{2/6}), 126.46 (2C, Ph'-C₁), 128.10 (4C, Ph'-C_{2/6}), 128.87 (4C, Ph'-C_{3/5}), 138.40 (2C, Ph'-C₄), 159.04 (Ph-C₁), 160.22 (2C, Ph-C_{3/5}). MS (ESI+) = *m/e* = 335.1 [M + 1]⁺.

Step II, Synthesis of 21b (O-(3,5-Diphenethoxyphenyl)dimethylcarbamothioate)¹⁴. Method A: NaH (95%, 0.16 g, 6.3 mmol), E₁, 21a (1.7 g, 5.1 mmol); E₂, dimethylthiocarbonyl chloride (0.62 g, 5.1 mmol); temperature, 60 °C; duration of synthesis, 5 h; product, transparent oil; yield, 65.4% (1.4 g). ¹H NMR (300.13 MHz, CDCl₃): δ = 3.03–3.11 (t, 4H, J = 6.8 Hz, Ph'-CH₂), 3.31 + 3.39 (s, 6H, N-CH₃), 4.11–4.23 (m, 4H, Ph-O-CH₂), 5.97–6.00 (m, 1H, Ph-H), 6.24–6.35 (m, 3H, Ph-H), 7.24–7.37 (m, 10H, Ph'-H). ¹³C NMR (75.44 MHz, CDCl₃): δ = 35.35 (2C, Ph'-CH₂), 38.70 (2C, N-CH₃), 68.82 (2C, Ph-O-CH₂), 98.85 (Ph-C₄), 101.02 (2C, Ph-C_{2/6}), 126.47 (2C, Ph'-C₄), 128.46 (4C, Ph'-C_{2/6}), 128.97 (4C, Ph'-C_{3/5}), 138.12 (2C, Ph'-C₁), 153.00 (Ph-C₁), 160.01 (2C, Ph-C_{3/5}), 187.42 (O-C-S). MS (ESI+) = *m/e* = 422.3 [M + 1]⁺.

Step III, Synthesis of 21c (S-(3,5-Diphenethoxyphenyl)dimethylcarbamothioate): In this step, a Newman–Kwart rearrangement was done to introduce the thiol group.¹⁴ Precursor 21b (1.4 g, 3.3 mmol) was heated to 240 °C (solvent-free) and stirred for 5 h. The transparent oil turns into a dark brown solution. Purification of the crude product (silica gel column chromatography; solvents *n*-hexane and ethyl acetate) yielded the pure compound as yellow oil. Yield: 43.6% (0.61 g). ¹H NMR (300.13 MHz, (CD₃)₂SO): δ = 2.87–3.01 (m, 10H, N-CH₃ + Ph'-CH₂), 4.07–4.18 (m, 4H, Ph-O-CH₂), 6.23 (d, 1H, Ph-H), 6.52–6.57 (m, 2H, Ph-H), 7.17–7.30 (m, 10H, Ph'-H). ¹³C NMR (75.44 MHz, (CD₃)₂SO): δ = 34.78 (2C, Ph'-CH₂), 36.41 (N-CH₃), 67.89 (2C, Ph-O-CH₂), 102.08 (Ph-C₄), 113.63 (2C, Ph-C_{2/6}), 126.23 (2C, Ph'-C₄), 128.25 (4C, Ph'-C_{2/6}), 128.90 (4C, Ph'-C_{3/5}), 138.24 (2C, Ph'-C₁), 159.31 (2C, Ph-C_{3/5}), 159.50 (Ph-C₁), 164.63 (C=S). MS (ESI+) = *m/e* = 422.3 [M + 1]⁺.

Step IV, Synthesis of 21d (3,5-Diphenethoxybenzenethiol): For deprotection of the thiol,¹⁴ 21c (0.6 g, 1.42 mmol) was dissolved in a mixture of THF and MeOH. After the mixture was heated at 80 °C, NaOH (1 mol/L, 10 mL) was added, and the solution was stirred for 3 h. Purification of the product was done with silica gel column chromatography yielding the product as milky oil in 50.2% yield (0.25 g). ¹H NMR (300.13 MHz, (CD₃)₂SO): δ = 3.02–3.07 (t, 4H, J = 6.7 Hz, Ph'-CH₂), 4.15–4.21 (t, 4H, J = 6.8 Hz, Ph-O-CH₂), 5.40 (s, 2H, -SH), 6.28–6.30 (m, 1H, Ph-H), 6.50–6.51 (m, 2H, Ph-H), 7.23–7.40 (m, 10H, Ph'-CH₂). MS (ESI-) = *m/e* = 349.1 [M - 1]⁻.

Step V, Synthesis of 21e (Ethyl 2-[(3,5-Diphenethoxyphenyl)thio]hexanoate): Method A: NaH (95%, 0.02 g, 0.85 mmol); E₁, 21d (0.25 g, 0.71 mmol); E₂, α-bromo ethylhexanoate (0.19 g, 0.85 mmol); duration of synthesis, 3 h; product, transparent oil; yield, 51.3% (0.18 g). ¹H NMR (300.13 MHz, (CD₃)₂SO): δ = 0.80–0.84 (t, 3H, J = 7.0 Hz, Bu-CH₃), 1.02–1.06 (t, 3H, J = 7.1 Hz, Et-CH₃), 1.23–1.37 (m, 4H, Bu-CH₂), 1.62–1.79 (m, 2H, Bu-CH₂), 2.96–3.00 (t, 4H, J = 6.8 Hz, Ph'-CH₂), 3.86–3.90 (t, 1H, J = 6.5 Hz, S-CH), 3.98–4.05 (q, 2H, J = 6.3 Hz,

O-CH₂), 4.12–4.17 (t, 4H, J = 6.8 Hz, Ph-O-CH₂), 6.38–6.39 (m, 1H, Ph-H), 6.51 (d, 2H, J = 2.1 Hz, Ph-H), 7.17–7.30 (m, 10H, Ph'-H). ¹³C NMR (75.44 MHz, (CD₃)₂SO): δ = 13.67 (Bu-CH₃), 13.84 (Et-CH₃), 21.67 (Bu-CH₂), 28.63 (Bu-CH₂), 30.80 (Bu-CH₂), 34.78 (2C, Ph'-CH₂), 48.83 (S-CH), 60.64 (O-CH₂), 68.27 (2C, Ph-O-CH₂), 100.29 (Ph-C₄), 108.98 (2C, Ph-C_{2/6}), 126.23 (2C, Ph'-C₄), 128.24 (4C, Ph'-C_{2/6}), 128.89 (4C, Ph'-C_{3/5}), 135.48 (Ph-C₁), 138.23 (2C, Ph'-C₁), 159.58 (2C, Ph-C_{3/5}), 171.62 (COO-). MS (ESI+) = *m/e* = 493.3 [M + 1]⁺.

Step VI, Synthesis of Final Compound 21 (2-[(3,5-Diphenethoxyphenyl)thio]hexanoic Acid): The corresponding ester 21e (0.13 g, 0.26 mmol) was dissolved in a mixture of 5 mL of THF/10 mL of MeOH and a solution of LiOH·H₂O (0.05 g, 1.31 mmol) in 3 mL of H₂O was added. After stirring at 50 °C for 3 h, the solvent was removed, and the residue was dissolved in water (under heating; if necessary, low amounts of MeOH were added). The solution was acidified with diluted hydrochloric acid. The formed precipitate was filtered, washed to neutrality with water, and then washed with *n*-hexane. Purification of the product was done using silica gel column chromatography and *n*-hexane/ethyl acetate to obtain the pure product as light yellow oil. Yield: 65.6% (0.12 g). ¹H NMR (300.13 MHz, (CD₃)₂SO): δ = 0.82–0.87 (t, 3H, J = 7.0 Hz, Bu-CH₃), 1.24–1.41 (m, 4H, Bu-CH₂), 1.58–1.84 (m, 2H, Bu-CH₂), 2.98–3.04 (t, 4H, J = 6.5 Hz, Ph'-CH₂), 3.77–3.83 (t, 1H, J = 7.0 Hz, S-CH), 4.14–4.19 (t, 4H, J = 6.7 Hz, Ph-O-CH₂), 6.37–6.41 (m, 1H, Ph-H), 6.53–6.56 (m, 2H, Ph-H), 7.19–7.33 (m, 10H, Ph'-H), 12.75 (s/br, 1H, COOH). ¹³C NMR (75.44 MHz, (CD₃)₂SO): δ = 13.70 (Bu-CH₃), 21.72 (Bu-CH₂), 28.71 (Bu-CH₂), 31.01 (Bu-CH₂), 34.82 (2C, Ph'-CH₂), 49.09 (S-CH), 68.26 (2C, Ph-O-CH₂), 99.96 (Ph-C₄), 108.46 (2C, Ph-C_{2/6}), 126.24 (2C, Ph'-C₄), 128.26 (4C, Ph'-C_{2/6}), 128.91 (4C, Ph'-C_{3/5}), 136.30 (Ph-C₁), 138.24 (2C, Ph'-C₁), 159.61 (2C, Ph-C_{3/5}), 173.06 (COO). MS (ESI+) = *m/e* = 465.5 [M + 1]⁺.

Synthesis of Compounds 23 and 24 (Exemplary of All Compounds with Central Carbon Scaffold (23–37))¹⁵.

Step I, Synthesis of Precursor A (Ethyl 2-(Diethylphosphoryl)hexanoate): Triethylphosphite and α-bromo ethylhexanoate were solved together. After stirring overnight at 120 °C, the mixture was distilled. First, the resulting ethylbromide was removed at 40 °C. Next, the product was distilled under vacuum (0.5 mbar) and 100 °C. ¹H NMR (300.13 MHz, (CD₃)₂SO): δ = 0.81–0.85 (t, 3H, J = 7.1 Hz, Bu-CH₃), 1.15–1.24 (m, 13H, Et-CH₃ + Bu-CH₂), 1.61–1.82 (m, 2H, Bu-CH₂), 2.91–3.04 (m, 1H, CH-COO-), 3.94–4.16 (m, 6H, O-CH₂). MS (ESI+) = *m/e* = 281.1 [M + 1]⁺.

Step IIa, Synthesis of 23b (3,5-Diphenethoxybenzaldehyde): 3, 5-Dihydroxybenzaldehyde (0.88 g, 6.34 mmol, 1 equiv), 2-phenylethanol (1.55 g, 12.7 mmol, 2.1 equiv), and triphenylphosphine (TPP; 3.66 g, 13.9 mmol, 2.5 equiv) were dissolved in anhydrous THF and stirred under argon atmosphere with ice bath cooling. 1,1'-(Azodicarbonyl)dipiperidine (ADDP; 3.36 g, 13.3 mmol, 2.5 equiv), diluted in 5 mL of THF, was added dropwise via a syringe, and the solution was stirred for 36 h. Subsequently, THF was evaporated, and the remaining residue was purified by silica gel column chromatography using *n*-hexane/ethyl acetate to yield the pure product as transparent oil. Yield: 54.7% (1.2 g). ¹H NMR (300.13 MHz, (CD₃)₂SO): δ = 3.42–3.47 (t, 3H, J = 6.8 Hz, Ph'-CH₂), 4.64–4.68 (t, 3H, J = 6.8 Hz, Ph-O-CH₂), 7.20–7.21 (d, 1H, J = 2.2 Hz, Ph-H), 7.45–7.46 (d, 2H, J = 5.3 Hz, Ph-H), 7.62–7.65 (m, 2H, Ph'-H), 7.66–7.75 (m, 8H, Ph'-H), 10.29 (s, 1H, CHO). ¹³C NMR (75.44 MHz, (CD₃)₂SO): δ = 35.19 (2C, Ph'-CH₂), 68.98 (2C, Ph-O-CH₂), 107.74 (Ph-C₄), 108.01 (2C, Ph-C_{2/6}), 126.70 (2C, Ph'-C₄), 128.71 (4C, Ph'-C_{2/6}), 129.35 (4C, Ph'-C_{3/5}), 138.60 (2C, Ph'-C₁), 138.64 (Ph-C₁), 160.49 (2C, Ph-C_{3/5}), 193.18 (CHO). MS (ESI+) = *m/e* = 361.2 [M + OH]⁺.

Step III, Synthesis of 23c (Ethyl 2-(3,5-Diphenethoxybenzylidene)hexanoate): Sodium hydride (95%; 0.11 g, 4.3 mmol, 1.3 equiv) was suspended in anhydrous THF and stirred under argon atmosphere with

ice bath cooling. The precursor **A** (1.21 g, 4.3 mmol, 1.3 equiv; in 5 mL of THF) was added to the suspension via a syringe leading to a clear solution. After 1 h, **23b** (1 g, 2.9 mmol, 1 equiv; in 5 mL of THF) was added, and the solution was stirred at room temperature for 3 h until the aldehyde was completely converted to **23c** (TLC control). After completion of the reaction, THF was evaporated, and the remaining solid was diluted with ethyl acetate. The organic phase was washed with water two times, dried over MgSO_4 , and evaporated. The crude product was purified by column chromatography using *n*-hexane/ethyl acetate to yield **23c** as transparent oil. Yield: 89% (1.2 g). ^1H NMR (300.13 MHz, $(\text{CD}_3)_2\text{SO}$): δ = 0.76–0.81 (t, 3H, J = 7.1 Hz, Bu-CH₃), 1.20–1.40 (m, 5H, Et-CH₃ + Bu-CH₂), 1.43–1.50 (m, 2H, Bu-CH₂), 2.37–2.43 (m, 2H, Bu-CH₂), 2.97–3.02 (t, 4H, J = 6.8 Hz, Ph'-CH₂), 4.10–4.19 (m, 6H, Ph-O-CH₂ + O-CH₂), 6.48–6.52 (dd, 3H, J = 1.7; 9.2 Hz, Ph-H), 7.16–7.29 (m, 10H, Ph'-H), 7.45 (s, 1H, C=CH). ^{13}C NMR (75.44 MHz, $(\text{CD}_3)_2\text{SO}$): δ = 13.56 (Bu-CH₃), 13.91 (Et-CH₃), 22.01 (Bu-CH₂), 26.94 (Bu-CH₂), 30.91 (Bu-CH₂), 34.15 (2C, Ph'-CH₂), 60.40 (O-CH₂), 68.26 (2C, Ph-O-CH₂), 100.47 (Ph-C₄), 107.61 (2C, Ph-C_{2/6}), 126.22 (2C, Ph'-C₄), 128.22 (4C, Ph'-C_{2/6}), 128.89 (4C, Ph'-C_{3/5}), 133.47 (Ph-C₁), 137.49 (COO-C=CH), 138.22 (Ph-CH), 138.31 (2C, Ph'-C₁), 159.54 (2C, Ph-C_{3/5}), 167.33 (COO-). MS (ESI+) = m/e = 473.1 [M + 1]⁺.

Step IV, Synthesis of Compound 23d (Ethyl 2-(3,5-Diphenethoxybenzyl)hexanoate): For synthesis of compound **23**, the exocyclic double bond was hydrogenated by solid-phase catalysis. The precursor **23c** was diluted in ethanol, and 10% (weight) Pd/C was added to the solution. The mixture was placed in an autoclave, gassed with H₂, and stirred at 5 bar. After 24 h, hydrogenation was completed, and the product was filtered over Celite. The solvent was evaporated, and the product **23d** was used without further purification (quantitative yield). ^1H NMR (300.13 MHz, $(\text{CD}_3)_2\text{SO}$): δ = 0.78–0.83 (t, 3H, J = 7.1 Hz, Bu-CH₃), 1.01–1.06 (t, 3H, J = 7.0 Hz, Et-CH₃), 1.08–1.21 (m, 4H, Bu-CH₂), 1.30–1.48 (m, 2H, Bu-CH₂), 2.58–2.69 (m, 3H, Ph-CH₂ + CH-COO), 2.95–3.00 (t, 4H, J = 6.8 Hz, Ph'-CH₂), 3.91–3.99 (m, 2H, O-CH₂), 4.08–4.13 (t, 4H, J = 6.8 Hz, Ph-O-CH₂), 6.29 (s, 3H, Ph-H), 7.17–7.30 (m, 10H, Ph'-H). ^{13}C NMR (75.44 MHz, $(\text{CD}_3)_2\text{SO}$): δ = 13.97 (Bu-CH₃), 14.00 (Et-CH₃), 21.92 (Bu-CH₂), 28.92 (Bu-CH₂), 31.36 (Bu-CH₂), 32.65 (Prop-C₃), 34.88 (Ph'-CH₂), 46.54 (Prop-C₂), 59.51 (O-CH₂), 68.03 (2C, Ph-O-CH₂), 98.97 (Ph-C₄), 107.42 (2C, Ph-C_{2/6}), 126.18 (2C, Ph'-C₄), 128.21 (4C, Ph'-C_{2/6}), 128.89 (4C, Ph'-C_{3/5}), 138.35 (2C, Ph'-C₁), 141.55 (Ph-C₁), 159.35 (2C, Ph-C_{3/5}), 174.66 (COO-). MS (ESI+) = m/e = 475.3 [M + 1]⁺.

Step V, Synthesis of Final Compounds 23 and 24. The corresponding ester **23d** (0.4 g, 0.8 mmol) or **23c** (0.4 g, 0.8 mmol) was dissolved in 6 mL of THF/4 mL of MeOH and a solution of LiOH·H₂O (0.18 g, 4.2 mmol) in 3 mL of H₂O was added. The mixture was stirred at 50 °C until the hydrolysis was completed (TLC control). Next, the solvent was removed, and the residue was dissolved in water (under heating; if necessary, low amounts of MeOH were added). The solution was acidified with diluted hydrochloric acid. The resulting precipitate was filtered, washed to neutrality with water, and afterward washed with *n*-hexane. Purification of **23** was done by silica gel column chromatography using *n*-hexane and ethyl acetate to give the pure product (**23**) as transparent oil in 76.3% (0.28 g) yield. Compound **24** was purified by recrystallization using methanol and H₂O to give a white solid. Yield: 93.1% (0.35 g).

Compound 23 (2-(3,5-Diphenethoxybenzyl)hexanoic Acid): ^1H NMR (300.13 MHz, $(\text{CD}_3)_2\text{SO}$): δ = 0.79–0.84 (t, 3H, J = 7.1 Hz, Bu-CH₃), 1.14–1.23 (m, 4H, Bu-CH₂), 1.37–1.48 (m, 2H, Bu-CH₂), 2.48–2.73 (m, 3H, Ph-CH₂ + CH-COO), 2.96–3.01 (t, 4H, J = 6.8 Hz, Ph'-CH₂), 4.09–4.13 (t, 4H, J = 6.8 Hz, Ph-O-CH₂), 6.29–6.31 (m, 3H, Ph-H), 7.17–7.30 (m, 10H, Ph'-H). ^{13}C NMR (75.44 MHz, $(\text{CD}_3)_2\text{SO}$): δ = 13.79 (Bu-CH₃), 22.02 (Bu-CH₂), 28.86 (Bu-CH₂), 31.33 (Bu-CH₂), 32.67 (Prop-C₃), 34.91 (2C, Ph'-CH₂), 46.56

(Prop-C₂), 68.01 (2C, Ph-O-CH₂), 98.74 (Ph-C₄), 107.48 (2C, Ph-C_{2/6}), 126.20 (2C, Ph'-C₄), 128.24 (4C, Ph'-C_{2/6}), 128.90 (4C, Ph'-C_{3/5}), 138.34 (2C, Ph'-C₄), 141.95 (Ph-C₁), 159.60 (2C, Ph-C_{3/5}), 176.29 (COOH). MS (ESI+) = m/e = 447.5 [M + 1]⁺.

Compound 24 (2-(3,5-Diphenethoxybenzylidene)hexanoic Acid): ^1H NMR (300.13 MHz, $(\text{CD}_3)_2\text{SO}$): δ = 0.77–0.82 (t, 3H, J = 7.0 Hz, Bu-CH₃), 1.24–1.27 (m, 2H, Bu-CH₂), 1.29–1.40 (m, 2H, Bu-CH₂), 2.35–2.40 (m, 2H, Bu-CH₂), 2.98–3.03 (t, 4H, J = 6.8 Hz, Ph'-CH₂), 4.15–4.19 (t, 4H, J = 6.8 Hz, Ph-O-CH₂), 6.48–6.53 (dd, 3H, J = 1.7; 9.2 Hz, Ph-H), 7.20–7.28 (m, 10H, Ph'-H), 7.44 (s, 1H, C=CH), 12.0 (s/br, 1H, COOH). ^{13}C NMR (75.44 MHz, $(\text{CD}_3)_2\text{SO}$): δ = 13.64 (Bu-CH₃), 22.38 (Bu-CH₂), 27.03 (Bu-CH₂), 30.91 (Bu-CH₂), 34.85 (2C, Ph'-CH₂), 68.26 (2C, Ph-O-CH₂), 101.41 (Ph-C₄), 107.61 (2C, Ph-C_{2/6}), 126.25 (2C, Ph'-C₄), 128.26 (4C, Ph'-C_{2/6}), 128.92 (4C, Ph'-C_{3/5}), 134.19 (Ph-C₁), 137.25 (CH-COO), 137.47 (Ph-C=CH), 138.26 (2C, Ph'-C₄), 159.53 (2C, Ph-C_{3/5}), 169.04 (COOH). MS (ESI-) = m/e = 443.5 [M - 1]⁻.

Assay Systems. *Materials.* Pirinixic acid, arachidonic acid, calcium ionophore A23187, DTT, fMLP, LPS, and all other fine chemicals were from Sigma (Deisenhofen, Germany), unless stated otherwise. 13(S)-HpODE was from Cayman Chemical (Ann Arbor, Michigan, USA); adenosine deaminase (Ada) and HPLC solvents were from Merck (Darmstadt, Germany).

Cells and Cell Viability Assay. Human PMNL were freshly isolated from leukocyte concentrates obtained at the Blood Center of the University Hospital Tuebingen (Germany). In brief, venous blood was taken from healthy adult donors, and leukocyte concentrates were prepared by centrifugation at 4000 × *g* for 20 min at 20 °C. PMNL were immediately isolated by dextran sedimentation, centrifugation on Nycoprep cushions (PAA Laboratories, Linz, Austria), and hypotonic lysis of erythrocytes as described previously.³⁴ Cells were finally resuspended in phosphate-buffered saline pH 7.4 (PBS) containing 1 mg/mL glucose and 1 mM CaCl₂ (PGC buffer).

Human A549 cells were cultured in DMEM/high glucose (4.5 g/L) medium supplemented with heat-inactivated fetal calf serum (FCS, 10% v/v), penicillin (100 U/mL) and streptomycin (100 μg/mL) at 37 °C and 5% CO₂. After 20 h, cells were transferred into DMEM/high glucose with FCS (2% v/v), penicillin (100 U/mL), and streptomycin (100 μg/mL), stimulated with 2 ng/mL interleukin-1β (IL-1β), and cultured for another 24 h at 37 °C. Then, confluent cells were detached using 1 × trypsin/EDTA solution; cell viability was measured using the colorimetric thiazolyl blue tetrazolium bromide (MTT) dye reduction assay as described.³⁵ In brief, A549 cells (1 × 10⁴ cells/100 μL) in medium supplemented with FCS (10% v/v) and IL-1β (2 ng/mL) were plated into a 96-well microplate and incubated at 37 °C and 5% CO₂ with test compounds, or solvent (DMSO) for 24 h. MTT (20 μL, 5 mg/mL) was added, and the incubations were continued for 1 h. The formazan product was solubilized with sodium dodecylsulfate (10%, w/v in 20 mM HCl) overnight shaking. The absorbance of each sample was measured at 595 nm relative to that of vehicle (DMSO)-treated control cells using a multiwell scanning spectrophotometer (Victor³ plate reader, PerkinElmer, Rodgau-Juegesheim, Germany).

Determination of Product Formation by 5-LO, 15-LO, and 12-LO in Cell-Based Assays. For assays of intact cells stimulated with calcium ionophore A23187 or NaCl, 5 × 10⁶ freshly isolated PMNL were resuspended in 1 mL of PGC buffer. After preincubation with the compounds for 15 min at 37 °C, 5-LO product formation was started by addition of 2.5 μM A23187 and exogenous AA as indicated or 0.3 M NaCl was supplemented 3 min before addition of AA. After 10 min at 37 °C, the reaction was stopped with 1 mL of methanol, and 30 μL of 1 N HCl, 200 ng of PGB₁, and 500 μL of PBS were added. Formed 5-LO metabolites were extracted and analyzed by HPLC as described.³⁶ 5-LO product formation is expressed as nanograms of 5-LO products per 10⁶ cells, which includes LTB₄ and its all-trans isomers, 5(S),

12(S)-dihydroxy-6,10-*trans*-8,14-*cis*-eicosatetraenoic acid (5(S),12(S)-DiHETE), and 5(S)-hydro(peroxy)-6-*trans*-8,11,14-*cis*-eicosatetraenoic acid (5-H(p)ETE). Cysteinyl LTsC₄, D₄, and E₄ were not detected, and oxidation products of LTB₄ were not determined. 15(S)-H(p)ETE was analyzed as product of 15-LO and 12(S)-H(p)ETE as product of 12-LO. To assess 5-LO product formation in cells stimulated with fMLP, 2 × 10⁷ PMNL were resuspended in 1 mL of PGC buffer, primed with 1 μg/mL LPS for 10 min at 37 °C, and 0.3 U/mL Ada was added. After another 10 min, cells were treated with the compounds for 10 min and 1 μM fMLP was added. The reaction was stopped on ice after 5 min, and cells were centrifuged (800 × g, 10 min). Formed LTB₄ was determined by ELISA according to the manufacturer's protocol (Assay Designs, Ann Arbor, MI).

Expression and Purification of Human Recombinant 5-LO from *Escherichia coli* and Determination of 5-LO Activity in Cell-Free Systems. *E. coli* BL21 was transformed with pT3-SLO plasmid, recombinant 5-LO protein was expressed at 37 °C, and 5-LO was purified as described.³³ Purified 5-LO was immediately used for 5-LO activity assays. For determination of 5-LO activity in corresponding supernatants of PMNL homogenates, 5 × 10⁶ freshly isolated PMNL were resuspended in 1 mL of PBS containing 1 mM EDTA and sonicated (3 × 10 s). Cell homogenates were centrifuged at 100 000 × g for 1 h at 4 °C to obtain 100 000 × g supernatants (S100). For determination of the activity of recombinant 5-LO, 0.5 μg of partially purified 5-LO was diluted with PBS/EDTA. Aliquots of S100 or purified 5-LO (0.5 μg) were diluted with PBS/EDTA plus 1 mM ATP, with or without 1 mM DTT, to 1 mL and preincubated with the test compounds. After 5–10 min at 4 °C, samples were prewarmed for 30 s at 37 °C, and 2 mM CaCl₂ and 20 μM AA, with or without 13(S)-HpODE, were added to start 5-LO product formation. The reaction was stopped after 10 min at 37 °C by addition of 1 mL of ice-cold methanol, and the formed metabolites were analyzed by HPLC as described for intact cells.

Induction of mPGES-1 in A549 Cells, Isolation of Microsomes, and Determination of PGE₂ Synthase Activity in Microsomes of A549 Cells. Preparation of human A549 cells was performed as described.^{37–39} In brief, cells (2 × 10⁶/20 mL DMEM/high glucose (4.5 g/L) medium containing FCS (2%, v/v)) were incubated for 16 h at 37 °C and 5% CO₂. Subsequently, the culture medium was replaced by fresh medium, IL-1β (1 ng/mL) was added, and cells were incubated for another 72 h. Thereafter, cells were detached with trypsin/EDTA, washed with PBS and frozen in liquid nitrogen. Ice-cold homogenization buffer (0.1 M potassium phosphate buffer, pH 7.4, 1 mM phenylmethylsulfonyl fluoride, 60 μg/mL soybean trypsin inhibitor, 1 μg/mL leupeptin, 2.5 mM glutathione, and 250 mM sucrose) was added, and after 15 min, cells were resuspended and sonicated on ice (3 × 20 s). The homogenate was subjected to differential centrifugation at 10 000 × g for 10 min and at 174 000 × g for 1 h at 4 °C. The pellet (microsomal fraction) was resuspended in 1 mL of homogenization buffer, and the protein concentration was determined by the Coomassie protein assay. The microsomal membranes were then diluted in potassium phosphate buffer (0.1 M, pH 7.4) containing 2.5 mM glutathione (100 μL total volume), and test compounds or vehicle (DMSO) was added. After 15 min, PGE₂ formation was initiated by addition of PGH₂ (20 μM, final concentration). After 1 min at 4 °C, the reaction was terminated with 100 μL of stop solution (40 mM FeCl₂, 80 mM citric acid, and 10 μM of 11β-PGE₂), PGE₂ was separated by solid-phase extraction on reversed-phase (RP)-C18 material using acetonitrile (200 μL) as eluent and analyzed by RP-HPLC (30% acetonitrile aqueous + 0.007% TFA (v/v), Nova-Pak C18 column, 5 × 100 mm², 4 μm particle size, flow rate 1 mL/min) with UV detection at 195 nm. 11β-PGE₂ was used as internal standard to quantify PGE₂ product formation by integration of the area under the peaks.

Determination of COX Inhibition. Inhibition of the activities of isolated ovine COX-1 and human recombinant COX-2 was performed as described.¹⁰ Briefly, purified COX-1 (ovine, 50 units) or COX-2 (human recombinant, 20 units) was diluted in 1 mL of reaction mixture containing 100 mM Tris buffer, pH 8, 5 mM glutathione, 5 μM hemoglobin, and 100 μM EDTA at 4 °C and preincubated with the test compounds for 5 min. Samples were prewarmed for 60 s at 37 °C, and AA (5 μM for COX-1, 2 μM for COX-2) was added to start the reaction. After 5 min at 37 °C, the COX product 12(S)-hydroxy-5-*cis*-8,10-*trans*-heptadecatrienoic acid (12-HHT) was extracted and then analyzed by HPLC as described.^{25,40}

Statistics. Data are expressed as mean ± SE. IC₅₀ values were calculated by nonlinear regression using SigmaPlot 9.0 (Systat Software Inc., San Jose, USA) one site binding competition. Statistical evaluation of the data was performed by one-way ANOVA followed by a Bonferroni or Tukey–Kramer *post-hoc* test for multiple comparisons, respectively. A *p* value < 0.05 (*) was considered significant.

■ ASSOCIATED CONTENT

S Supporting Information. Chemical syntheses, ¹H and ¹³C NMR values of intermediates and final products, mass spectrometry, and combustion analysis. This material is available free of charge via the Internet at <http://pubs.acs.org>.

■ AUTHOR INFORMATION

Corresponding Author

*M.S.-Z.: phone +49-069-79829339; fax +49-69-79829332; e-mail schubert-zsilavec@pharmchem.uni-frankfurt.de. O.W.: phone +49-03641-949801; fax +49-03641-949802; e-mail oliver.werz@uni-jena.de.

Author Contributions

[†]These authors contributed equally to this study.

■ ACKNOWLEDGMENT

The authors thank Daniela Müller for expert technical assistance and Aurelianus GmbH/Tuebingen, Germany and the Doktor-Robert-Pfleger-Stiftung for financial support.

■ ABBREVIATIONS

AA, arachidonic acid; CLP, coactosine-like protein; COX, cyclooxygenase; cPLA₂, cytosolic phospholipase A₂; CVD, cardiovascular disease; DPPH, 1,1-diphenyl-2-picrylhydrazyl; fMLP, *N*-formyl-methionyl-leucyl-phenylalanine; FLAP, 5-lipoxygenase activating protein; LPS, lipopolysaccharide; 5-LO, 5-lipoxygenase; LT, leukotriene; mPGES-1, microsomal prostaglandin E₂ synthase-1; MAPK, mitogen-activated protein kinase; NSAID, nonsteroidal anti-inflammatory drug; PG, prostaglandin; PGC buffer, phosphate-buffered saline, pH 7.4, containing 1 mg/mL glucose and 1 mM CaCl₂; PMNL, polymorphonuclear leukocyte; SAR, structure–activity relationship; q.s., quantum satis, meaning the amount that is needed

■ REFERENCES

- (1) Radmark, O.; Samuelsson, B. Microsomal prostaglandin E synthase-1 and 5-lipoxygenase: Potential drug targets in cancer. *J. Intern. Med.* **2010**, *268*, 5–14.
- (2) Peters-Golden, M.; Henderson, W. R., Jr. Leukotrienes. *N. Engl. J. Med.* **2007**, *357*, 1841–1854.

- (3) Wang, D.; DuBois, R. Eicosanoids and cancer. *Nat. Rev. Cancer* **2010**, *10*, 181–193.
- (4) Rainsford, K. D. Anti-inflammatory drugs in the 21st century. *Subcell. Biochem.* **2007**, *42*, 3–27.
- (5) Celotti, F.; Laufer, S. Anti-inflammatory drugs: New multitarget compounds to face an old problem. The dual inhibition concept. *Pharmacol. Res.* **2001**, *43*, 429–436.
- (6) Radmark, O.; Werz, O.; Steinhilber, D.; Samuelsson, B. 5-Lipoxygenase: Regulation of expression and enzyme activity. *Trends Biochem. Sci.* **2007**, *32*, 332–341.
- (7) Werz, O.; Steinhilber, D. Development of 5-lipoxygenase inhibitors—lessons from cellular enzyme regulation. *Biochem. Pharmacol.* **2005**, *70*, 327–333.
- (8) Feisst, C.; Pergola, C.; Rakonjac, M.; Rossi, A.; Koeberle, A.; Dodt, G.; Hoffmann, M.; Hoernig, C.; Fischer, L.; Steinhilber, D.; Franke, L.; Schneider, G.; Radmark, O.; Sautebin, L.; Werz, O. Hyperforin is a novel type of 5-lipoxygenase inhibitor with high efficacy in vivo. *Cell. Mol. Life Sci.* **2009**, *66*, 2759–2771.
- (9) Werz, O. 5-Lipoxygenase: Cellular biology and molecular pharmacology. *Curr. Drug Targets: Inflammation Allergy* **2002**, *1*, 23–44.
- (10) Koeberle, A.; Zettl, H.; Greiner, C.; Wurglics, M.; Schubert-Zsilavecz, M.; Werz, O. Pirinixic acid derivatives as novel dual inhibitors of microsomal prostaglandin E2 synthase-1 and 5-lipoxygenase. *J. Med. Chem.* **2008**, *51*, 8068–8076.
- (11) Koeberle, A.; Rossi, A.; Zettl, H.; Pergola, C.; Dehm, F.; Bauer, J.; Greiner, C.; Reckel, S.; Hoernig, C.; Northoff, H.; Bernhard, F.; Dotsch, V.; Sautebin, L.; Schubert-Zsilavecz, M.; Werz, O. The molecular pharmacology and in vivo activity of 2-(4-chloro-6-(2,3-dimethylphenylamino)pyrimidin-2-ylthio)octanoic acid (YS121), a dual inhibitor of microsomal prostaglandin E2 synthase-1 and 5-lipoxygenase. *J. Pharmacol. Exp. Ther.* **2010**, *332*, 840–848.
- (12) Hieke, M.; Ness, J.; Steri, R.; Dittrich, M.; Greiner, C.; Werz, O.; Baumann, K.; Schubert-Zsilavecz, M.; Weggen, S.; Zettl, H. Design, synthesis, and biological evaluation of a novel class of γ -secretase modulators with PPAR γ activity. *J. Med. Chem.* **2010**, *53*, 4691–4700.
- (13) Bharate, S. B.; Khan, S. I.; Yunus, N. A.; Chauthe, S. K.; Jacob, M. R.; Tekwani, B. L.; Khan, I. A.; Singh, I. P. Antiprotozoal and antimicrobial activities of O-alkylated and formylated acylphloroglucinols. *Bioorg. Med. Chem.* **2007**, *15*, 87–96.
- (14) Yoshida, Y.; Barrett, D.; Azami, H.; Morinaga, C.; Matsumoto, S.; Matsumoto, Y.; Takasugi, H. Studies on anti-*Helicobacter pylori* agents. Part 1: Benzyloxyisoquinoline derivatives. *Bioorg. Med. Chem.* **1999**, *7*, 2647–2666.
- (15) Zettl, H.; Steri, R.; Lämmerhofer, M.; Schubert-Zsilavecz, M. Discovery of a novel class of 2-mercaptohexanoic acid derivatives as highly active PPAR α agonists. *Bioorg. Med. Chem. Lett.* **2009**, *19*, 4421–4426.
- (16) Karg, E. M.; Luderer, S.; Pergola, C.; Buhning, U.; Rossi, A.; Northoff, H.; Sautebin, L.; Troschutz, R.; Werz, O. Structural optimization and biological evaluation of 2-substituted 5-hydroxyindole-3-carboxylates as potent inhibitors of human 5-lipoxygenase. *J. Med. Chem.* **2009**, *52*, 3474–3483.
- (17) Koeberle, A.; Siemoneit, U.; Buhning, U.; Northoff, H.; Laufer, S.; Albrecht, W.; Werz, O. Licofelone suppresses prostaglandin E2 formation by interference with the inducible microsomal prostaglandin E2 synthase-1. *J. Pharmacol. Exp. Ther.* **2008**, *326*, 975–982.
- (18) Siemoneit, U.; Hofmann, B.; Kather, N.; Lamkemeyer, T.; Madlung, J.; Franke, L.; Schneider, G.; Jauch, J.; Poeckel, D.; Werz, O. Identification and functional analysis of cyclooxygenase-1 as a molecular target of boswellic acids. *Biochem. Pharmacol.* **2008**, *75*, 503–513.
- (19) Tateson, J. E.; Randall, R. W.; Reynolds, C. H.; Jackson, W. P.; Bhattacharjee, P.; Salmon, J. A.; Garland, L. G. Selective inhibition of arachidonate 5-lipoxygenase by novel acetohydroxamic acids: biochemical assessment in vitro and ex vivo. *Br. J. Pharmacol.* **1988**, *94*, 528–539.
- (20) Claveau, D.; Sirinyan, M.; Guay, J.; Gordon, R.; Chan, C. C.; Bureau, Y.; Riendeau, D.; Mancini, J. A. Microsomal prostaglandin E synthase-1 is a major terminal synthase that is selectively up-regulated during cyclooxygenase-2-dependent prostaglandin E2 production in the rat adjuvant-induced arthritis model. *J. Immunol.* **2003**, *170*, 4738–4744.
- (21) Werz, O.; Szellas, D.; Henseler, M.; Steinhilber, D. Nonredox 5-lipoxygenase inhibitors require glutathione peroxidase for efficient inhibition of 5-lipoxygenase activity. *Mol. Pharmacol.* **1998**, *54*, 445–451.
- (22) Werz, O.; Burkert, E.; Fischer, L.; Szellas, D.; Dishart, D.; Samuelsson, B.; Radmark, O.; Steinhilber, D. 5-Lipoxygenase activation by MAPKAPK-2 and ERKs. *Adv. Exp. Med. Biol.* **2003**, *525*, 129–132.
- (23) Pergola, C.; Dodt, G.; Rossi, A.; Neunhoeffer, E.; Lawrenz, B.; Northoff, H.; Samuelsson, B.; Radmark, O.; Sautebin, L.; Werz, O. ERK-mediated regulation of leukotriene biosynthesis by androgens: A molecular basis for gender differences in inflammation and asthma. *Proc. Natl. Acad. Sci. U.S.A.* **2008**, *105*, 19881–19886.
- (24) Werz, O.; Burkert, E.; Samuelsson, B.; Radmark, O.; Steinhilber, D. Activation of 5-lipoxygenase by cell stress is calcium independent in human polymorphonuclear leukocytes. *Blood* **2002**, *99*, 1044–1052.
- (25) Teixeira, M. M.; Hellewell, P. G. Effect of a 5-lipoxygenase inhibitor, ZM 230487, on cutaneous allergic inflammation in the guinea-pig. *Br. J. Pharmacol.* **1994**, *111*, 1205–1211.
- (26) Berman, H. M.; Westbrook, J.; Feng, Z.; Gilliland, G.; Bhat, T. N.; Weissig, H.; Shindyalov, I. N.; Bourne, P. E. The Protein Data Bank. *Nucleic Acids Res.* **2000**, *28*, 235–242.
- (27) Gilbert, N. C.; Bartlett, S. G.; Waight, M. T.; Neau, D. B.; Boeglin, W. E.; Brash, A. R.; Newcomer, M. E. The structure of human 5-lipoxygenase. *Science* **2011**, *331*, 217–219.
- (28) Jegerschold, C.; Pawelzik, S. C.; Purhonen, P.; Bhakat, P.; Gheorghe, K. R.; Gyobu, N.; Mitsuoka, K.; Morgenstern, R.; Jakobsson, P. J.; Hebert, H. Structural basis for induced formation of the inflammatory mediator prostaglandin E2. *Proc. Natl. Acad. Sci. U.S.A.* **2008**, *105*, 11110–11115.
- (29) Weisel, M.; Proschak, E.; Schneider, G. PocketPicker: Analysis of ligand binding-sites with shape descriptors. *Chem. Cent. J.* **2007**, *1* No. 7.
- (30) Paul, N.; Kellenberger, E.; Bret, G.; Muller, P.; Rognan, D. Recovering the true targets of specific ligands by virtual screening of the protein data bank. *Proteins* **2004**, *54*, 671–680.
- (31) Reisen, F.; Weisel, M.; Kriegl, J. M.; Schneider, G. Self-organizing fuzzy graphs for structure-based comparison of protein pockets. *J. Proteome Res.* **2010**, *9*, 6498–6510.
- (32) Jones, G.; Willett, P.; Glen, R. C. Molecular recognition of receptor sites using a genetic algorithm with a description of desolvation. *J. Mol. Biol.* **1995**, *245*, 43–53.
- (33) Fischer, L.; Szellas, D.; Radmark, O.; Steinhilber, D.; Werz, O. Phosphorylation- and stimulus-dependent inhibition of cellular 5-lipoxygenase activity by nonredox-type inhibitors. *FASEB J.* **2003**, *17*, 949–951.
- (34) Albert, D.; Zundorf, I.; Dinger, T.; Müller, W. E.; Steinhilber, D.; Werz, O. Hyperforin is a dual inhibitor of cyclooxygenase-1 and 5-lipoxygenase. *Biochem. Pharmacol.* **2002**, *64*, 1767–1775.
- (35) Tretiakova, I.; Blaesus, D.; Maxia, L.; Wesselborg, S.; Schulze-Osthoff, K.; Cinatl, J., Jr.; Michaelis, M.; Werz, O. Myrtilin from *Myrtus communis* induces apoptosis in cancer cells via the mitochondrial pathway involving caspase-9. *Apoptosis* **2008**, *13*, 119–131.
- (36) Werz, O.; Szellas, D.; Steinhilber, D.; Radmark, O. Arachidonic acid promotes phosphorylation of 5-lipoxygenase at Ser-271 by MAPK-activated protein kinase 2 (MK2). *J. Biol. Chem.* **2002**, *277*, 14793–14800.
- (37) Jakobsson, P. J.; Thoren, S.; Morgenstern, R.; Samuelsson, B. Identification of human prostaglandin E synthase: A microsomal, glutathione-dependent, inducible enzyme, constituting a potential novel drug target. *Proc. Natl. Acad. Sci. U.S.A.* **1999**, *96*, 7220–7225.
- (38) Werz, O.; Greiner, C.; Koeberle, A.; Hoernig, C.; George, S.; Popescu, L.; Syha, I.; Schubert-Zsilavecz, M.; Steinhilber, D. Novel and potent inhibitors of 5-lipoxygenase product synthesis based on the structure of pirinixic acid. *J. Med. Chem.* **2008**, *51*, 5449–5453.

(39) Popescu, L.; Rau, O.; Bottcher, J.; Syha, Y.; Schubert-Zsilavecz, M. Quinoline-based derivatives of pirinixic acid as dual PPAR alpha/gamma agonists. *Arch. Pharm. (Weinheim, Ger.)* **2007**, *340*, 367–371.

(40) Kato, M.; Nishida, S.; Kitasato, H.; Sakata, N.; Kawai, S. Cyclooxygenase-1 and cyclooxygenase-2 selectivity of non-steroidal anti-inflammatory drugs: investigation using human peripheral monocytes. *J. Pharm. Pharmacol.* **2001**, *53*, 1679–1685.